Molecular Biology of the Cell
Vol. 15, 4148–4165, September 2004

The Basolateral Targeting Signal of CD147 (EMMPRIN) Consists of a Single Leucine and Is Not Recognized by Retinal Pigment Epithelium[D]

Ami A. Deora,* Diego Gravotta,* Geri Kreitzer,† Jane Hu,‡ Dean Bok,‡§‖ and Enrique Rodriguez-Boulan*¶

*Margaret M. Dyson Vision Research Institute, Department of Ophthalmology, †Department of Cell and Developmental Biology, Weill Medical College of Cornell University, New York, NY 10021; and ‡Jules Stein Eye Institute, §Brain Research Institute, and ‖Department of Neurobiology, School of Medicine, University of California, Los Angeles, CA 90095

Submitted January 21, 2004; Revised May 28, 2004; Accepted June 14, 2004
Monitoring Editor: Juan S. Bonifacino

CD147, a type I integral membrane protein of the immunoglobulin superfamily, exhibits reversed polarity in retinal pigment epithelium (RPE). CD147 is apical in RPE in contrast to its basolateral localization in extraocular epithelia. This elicited our interest in understanding the basolateral sorting signals of CD147 in prototypic Madin-Darby canine kidney (MDCK) cells. The cytoplasmic domain of CD147 has basolateral sorting information but is devoid of well-characterized basolateral signals, such as tyrosine and di-leucine motifs. Hence, we carried out systematic site-directed mutagenesis to delineate basolateral targeting information in CD147. Our detailed analysis identified a single leucine (252) as the basolateral targeting motif in the cytoplasmic tail of CD147. Four amino acids (243–246) N-terminal to leucine 252 are also critical basolateral determinants of CD147, because deletion of these amino acids leads to mistargeting of CD147 to the apical membranes. We ruled out the involvement of adaptor complex 1B (AP1B) in the basolateral trafficking of CD147, because LLC-PK1 cells lacking AP1B, target CD147 basolaterally. At variance with MDCK cells, the human RPE cell line ARPE-19 does not distinguish between CD147 (WT) and CD147 with leucine 252 mutated to alanine and targets both proteins apically. Thus, our study identifies an atypical basolateral motif of CD147, which comprises a single leucine and is not recognized by RPE cells. This unusual basolateral sorting signal will be useful in unraveling the specialized sorting machinery of RPE cells.

INTRODUCTION

Epithelial cells have distinct apical and basolateral membrane domains with different protein and lipid compositions. The asymmetry is essential for the multiple vectorial functions they perform (Rodriguez-Boulan and Nelson, 1989; Yeaman *et al.*, 1999). The polarized protein distribution results from sorting mechanisms operating in the biosynthetic and recycling pathways that recognize specific sorting signals in plasma membrane proteins. Structural features believed to operate as apical sorting signals include glycosylphophatidylinositol anchors (Lisanti *et al.*, 1989), N-glycans (Scheiffele *et al.*, 1995), O-glycans (Yeaman *et al.*, 1997; Jacob *et al.*, 2000), and protein sequences in the transmembrane (Kundu *et al.*, 1996; Lin *et al.*, 1998), or cytoplasmic domains (Chuang and Sung, 1998; Rodriguez-Boulan and Gonzalez, 1999; Nelson and Yeaman, 2001). On the other hand, basolateral signals are formed by short peptide sequences usually found in the protein domain facing the cytosol (Le Gall *et al.*, 1995; Yeaman *et al.*, 1999; Mostov *et al.*, 2000). They mainly include tyrosine motifs (consensus motif NPXY or YXXF) as well as di-leucine and di-hydrophobic residues (Matter *et al.*, 1992; Aroeti *et al.*, 1993; Hunziker and Fumey, 1994; Simonsen *et al.*, 1997; Bonifacino and Dell'Angelica, 1999; Rodionov *et al.*, 2000).

Different types of epithelial cells vary widely in the final distribution of plasma membrane proteins or in the pathways that these proteins follow to the cell surface (Keller and Simons, 1997). Recently some mechanisms that could account for this variation have become evident. Adaptins have been identified that recognize tyrosine and di-leucine motifs and mediate protein sorting at specific subcellular organelles. Tyrosine-based sorting signals are mainly recognized by the medium (μ) subunit of heterotetrameric adaptors (AP1–4). In contrast, di-leucine–based sorting signals are recognized by monomeric Golgi-localized, gamma-ear–containing, Arf-binding (GGA) adaptors (Heilker *et al.*, 1999; Bonifacino and Traub, 2003). In some cases the expression of these adaptins may be tissue specific. Such is the case with AP1B, which contains an epithelial-specific μ1B subunit (Ohno *et al.*, 1999). LLC-PK1, a cell line originated from the proximal kidney tubule, does not express this subunit and as a consequence, missorts a subgroup of basolateral proteins to the apical surface (Roush *et al.*, 1998; Folsch *et al.*, 1999). Our past work suggests that AP1B operates in recycling

Article published online ahead of print. Mol. Biol. Cell 10.1091/mbc.E04–01–0058. Article and publication date are available at www.molbiolcell.org/cgi/doi/10.1091/mbc.E04–01–0058.

[D] Online version of this article contains supporting material. Online version is available at www.molbiolcell.org.

¶ Corresponding author. E-mail address: boulan@mail.med. cornell.edu.

Abbreviations used: MDCK, Madin-Darby canine kidney; RPE, retinal pigment epithelium; BL, basolateral; AP, apical; AP1B, adaptor complex 1B.

basolateral proteins from endosomes, rather than in biosynthetic sorting from the Golgi to the cell surface in LLC-PK1 cells (Gan *et al.*, 2002). However, a recent report by Folsch *et al.* (2003) suggests a role of AP1B in sorting basolateral proteins at an endosomal compartment in the biosynthetic pathway. It is not clear yet whether these different results reflect the different model proteins studied in each report. Expression of distinct complements of plasma membrane SNAP receptor (SNARE) fusion proteins may also be responsible for differences in the polarized protein distribution in various epithelia (Li *et al.*, 2002; Low *et al.*, 2002).

For various physiological reasons, retinal pigment epithelium (RPE) displays several plasma membrane proteins at the apical surface that are basolateral in extraocular epithelia (Zinn and Marmor, 1979; Marmor and Wolfensberger, 1998; Marmorstein, 2001). Examples of this behavior include Na,K-ATPase (Miller *et al.*, 1978; Okami *et al.*, 1990; Gundersen *et al.*, 1991), neural cell adhesion molecule (NCAM; Gundersen *et al.*, 1993), monocarboxylate transporter 1 (Philp *et al.*, 1998), and CD147 (Marmorstein *et al.*, 1996). CD147, a type I membrane protein and a member of the immunoglobulin superfamily (Stockinger *et al.*, 1997), has been independently cloned from different species and is also referred to as human EMMPRIN/M6 (Biswas *et al.*, 1995), mouse basigin (Miyauchi *et al.*, 1990), chicken 5A11 (Fadool and Linser, 1993a), avian HT7 (Seulberger *et al.*, 1992), and rat CE-9 (Nehme *et al.*, 1993). Mice with targeted disruption of the CD147 gene are blind starting 5 weeks after birth (Hori *et al.*, 2000) because of deficient photoreceptor development and retinal degeneration (Ochrietor *et al.*, 2001, 2002). Significantly, CD147 has a strong expression level in the retina, especially in the RPE (Neill and Barnstable, 1990; Fan *et al.*, 1998; Philp *et al.*, 2003). CD147 has also been implicated in important extraocular functions, such as development of the blood-brain barrier, neuronal-glial interactions, and leukocyte activation (Schlosshauer and Herzog, 1990; Kasinrerk *et al.*, 1992; Fadool and Linser, 1993b). Knockout mice show defects in embryogenesis, spermatogenesis, and female fertilization (Igakura *et al.*, 1998). It is likely that at least some of the functions of CD147 are related to its ability to stimulate matrix metalloproteinases (Biswas and Nugent, 1987).

In contrast to its basolateral distribution in extraocular epithelia, e.g., liver, thyroid, kidney (Bartles *et al.*, 1985; Finnemann *et al.*, 1997), the polarity of CD147 in RPE is developmentally regulated. From a predominantly basolateral localization in newborn rat RPE at postnatal day 1, it shifts to a nonpolar distribution at postnatal day 7 and to a predominantly apical localization in adult RPE (Marmorstein *et al.*, 1996). The shift of the bulk of CD147 from the basolateral to the apical membrane in maturing RPE coincides with maturation of photoreceptors and the interphotoreceptor matrix, suggesting a key role of CD147 in the maintenance of the neural retina. This polarity shift correlates with the expansion of the apical:basolateral surface ratio to the adult level of 3:1. Quantification of CD147 by using an eye-cup biotin polarity assay revealed accumulation of three times more CD147 in the apical than in the basolateral domain, suggesting that CD147 achieves apical distribution due to asymmetric growth of the adult RPE plasma membrane and not because of active apical sorting (Marmorstein *et al.*, 1998a). This led to the suggestion that maturing RPE cells cease to recognize the basolateral signal of CD147.

Identifying precisely the targeting domain of CD147 is crucial to understanding its basolateral location in extraocular epithelia and the mechanisms utilized by adult RPE cells to suppress recognition of CD147's basolateral signal. Our previous work has suggested that CD147 has dominant basolateral targeting information in the cytoplasmic tail, which is highly conserved across species and has a weak apical signal in the ectodomain (Marmorstein *et al.*, 1998a). The cytoplasmic domain of CD147 lacks typical tyrosine or di-hydrophobic consensus motifs. We constructed several cytoplasmic domain mutants of the C-terminal end by progressive truncation, internal deletions and point mutations to map the basolateral targeting signal of CD147 in the archetype polarized epithelial cell line MDCK. Our results identify an atypical basolateral determinant in CD147 that comprises a single leucine.

MATERIALS AND METHODS

Cell Culture

Madin-Darby canine kidney (MDCK) II cells were maintained in DMEM (Cellgro, Herndon, VA) supplemented with 10% fetal bovine serum (Gemini, Woodland, CA), 1% glutamine, and 1% penicillin/streptomycin (Cellgro) at 37°C in 95% air/5% CO_2 atmosphere. LLC-PK1 cells were maintained in DMEM supplemented with 5% fetal calf serum, 5% calf serum, glutamine, nonessential amino acids, and penicillin/streptomycin. Fisher rat thyroid (FRT) cells were grown in Ham's F12/Coon's modified media (Sigma, St. Louis, MO) supplemented with 5% fetal bovine serum. MDCK cells were plated on 12-mm (1-cm^2 area) Transwell polycarbonate filter units (0.4-μm pore size; Costar, Cambridge, MA) at a density of 250,000 cells/well and cultured for 5 days to allow development of polarity. The medium was changed every other day. Monolayers exhibiting transepithelial electrical resistance above 100 $\Omega \cdot cm^2$ were used for surface biotinylation and immunofluorescence microscopy. LLC-PK1 and FRT cells were also grown in similar manner on 12-mm Transwell polycarbonate filters. Human fetal RPE cells grown in Chee's essential replacement medium containing 1% bovine retinal extract (Hu and Bok, 2001) exhibit cell polarization and differentiation comparable to RPE in vivo. These cells were collected from eyes of human aborted fetuses of 21 weeks' gestation. The culture method for obtaining human RPE cells is as described previously (Frambach *et al.*, 1990; Hu *et al.*, 1994; Hu and Bok, 2001). The cells were grown on Millicell-PCF filters 0.4-μm pore size (12 mm; Millipore, Bedford, MA). The tenets of the Declaration of Helsinki were followed, and the patients (or their guardians) gave consent for donation of the tissue. Institutional Human Experimentation Committee approval was obtained for the use of human eyes. ARPE-19 cells, obtained from ATCC, are a spontaneously arising human RPE cell line that exhibits polarized characteristics when grown on laminin-coated filter supports. (Dunn *et al.*, 1996, 1998). Cells were grown in Chee's essential replacement medium containing 1% bovine retinal extract and polarized by growing on laminin (BD Biosciences, CA)-coated Transwell filters for 6 weeks (Alizadeh *et al.*, 2001). A plating density of 250,000 cells/cm^2 was used. The medium was changed twice a week. After 6 weeks, typical transepithelial electrical resistance measurements in ARPE-19 cells were ~50 $\Omega \cdot cm^2$.

Site-directed Mutagenesis of Cytoplasmic Tail of CD147 and Generation of Tac Chimeras

A QuikChange site-directed mutagenesis kit (Stratagene, La Jolla, CA) was used to introduce stop-codon, deletion, and substitutions in the CD147 cDNA (Rat CE-9, EMBL/GenBank accession no. X67215) in pcDNA3.1 vector (Invitrogen, Carlsbad, CA). The pairs of custom-synthesized complementary mutagenic oligonucleotides were obtained from Sigma-Genosys (Woodlands, TX). Different cytoplasmic domain CD147 constructs generated are detailed in Figure 2. To determine whether the extracellular domain of CD147 plays any role in basolateral targeting, a chimera of Tac (interleukin-2 receptor alpha chain) and CD147 was generated. Tac-CD147 chimera comprises the extracellular domain of Tac, and transmembrane and cytoplasmic domains of CD147. To generate the Tac-CD147 chimera, a *Bgl*II site was generated upstream of the transmembrane domain of CD147. The transmembrane and cytoplasmic domains of CD147 were swapped at a unique *Bgl*II site in Tac located upstream of the transmembrane sequences of Tac. All the constructs were subsequently sequenced to verify the intended mutation. DNA sequencing was performed by the BioResearch Center of Cornell University (Ithaca, NY).

Stable Transfection

MDCK II and LLC-PK1 cells were transfected with constructs of CD147 using Effectene (Qiagen, Hilden, Germany) according to the manufacturer's protocol. Stable clones were selected and maintained in a selection medium containing 500 μg/ml neomycin on the basis of protein levels monitored by

Western blotting and immunofluorescence. For each CD147 construct, at least three independent clones were used to assess polarity.

Transient Transfection of Polarized MDCK and ARPE-19 Cells

We utilized a recently improved technique to transfect polarized epithelial cells that relies on lipid reagents like Effectene (Tucker *et al.*, 2003). Briefly, polarized monolayers of MDCK and ARPE-19 cells grown on Transwells were washed three times with OptiMEM-I medium (Life Technologies, Rockville, MD). DNA-Effectene complex (containing 1 μg DNA, 6 μl enhancer, and 12 μl Effectene diluted in 1.5 ml OptiMEM-I) was added to both apical and basolateral sides. Cells were incubated with the DNA-Effectene complex for 6 h at 37°C. After 6 h, OptiMEM-I was replaced with regular serum containing medium. Monolayers were analyzed 48 h posttransfection by fixing cells in 2% paraformaldehyde (PFA). The transfection efficiency was 5–10%, and no cell toxicity was observed. Transepithelial resistance was identical in control vs. transfected cells. Immunostaining with E-cadherin (for MDCK cells) and endogenous CD147, β-catenin (for ARPE-19 cells) was also utilized to determine whether the monolayers were intact. We transfected MDCK and ARPE-19 monolayers with GFP-tagged constructs of CD147 (WT) and CD147 (L252A) (EGFP-N1 vector from Clontech, Palo Alto, CA). GFP-tag fused with the C-terminus of CD147 did not affect the trafficking of CD147 (see Supplementary Material). Additionally, we also used cDNA of Tac-CD147 (WT) and Tac-CD147(L252A) chimeras and stem cell factor (SCF-GFP; a kind gift from Dr. Bernhard Wehrle-Haller) for transfection.

Immunofluorescence Microscopy

Cells were fixed in 2% freshly prepared PFA in PBS for 20 min at room temperature and quenched with 50 mM NH_4Cl in PBS containing 1 mM $CaCl_2$, and 1 mM $MgCl_2$ (PBS/CM). Monolayers growing on Transwell filters were processed for immunofluorescence by adding antibody both to basal and apical sides of the filter. For permeabilization either methanol at −20°C or 0.075% saponin was used. Cells were blocked in PBS/CM containing 0.2% BSA. The following primary antibodies were used: mAb against the ectodomain of rat CD147 (1:1000 dilution; RET-PE2 hybridoma, kindly provided by Dr. Colin Barnstable), mouse anti-human CD147 (1:1000 dilution; BD Biosciences (Pharmingen), San Diego, CA), β-catenin antibody (1:1000 dilution; Sigma), E-cadherin (1:1000 dilution; Transduction Laboratories, Lexington, KY) and anti-Tac antibody (1:1000 dilution; Santa Cruz Biotechnology, Santa Cruz, CA). Secondary antibodies used were Alexa 488–tagged anti-mouse IgG and Alexa 568-tagged anti-rabbit IgG. TO-PRO-3 iodide was utilized for nuclear staining (Molecular Probes, Eugene, OR). RET-PE2 antibody exhibits no nonspecific staining in nontransfected MDCK cells. Immunostaining for CD147, Tac, and E-cadherin was performed on nonpermeabilized cells. After primary and secondary antibody incubations, cells were postfixed with 2% PFA and then permeabilized for staining of β-catenin and with TO-PRO-3 iodide. Images were obtained on a laser scanning confocal microscope (Carl Zeiss, Thornwood, NY) with a 63× oil objective. Serial (0.5 μm) *x-y* (en face) and *x-z* sections (top to bottom) were collected and processed with LSM510 software (Zeiss) and Adobe Photoshop 5.0 (San Jose, CA). Images presented here show individual confocal *x-y* section and the entire *x-z* section.

Domain-specific Cell Surface Biotinylation to Determine Steady State Polarity

We performed domain-selective biotinylation to measure steady state polarity of surface proteins as described previously (Le Bivic *et al.*, 1990; Marmorstein *et al.*, 1998b). Briefly, either the basal or apical side of the filter was exposed to cell impermeable sulfo-NHS-SS-biotin (0.5 mg/ml; Pierce, Rockford, IL) twice successively for 20 min at 4°C. The biotinylation reaction was quenched in PBS, containing 50 mM NH_4Cl for 10 min. Biotinylated cells were lysed in 1% Triton X-100 lysis buffer containing a protease inhibitor cocktail. Biotinylated proteins were captured on streptavidin-agarose beads; after the beads were washed and pelleted, the biotinylated proteins were analyzed by SDS-PAGE, blotted onto a nitrocellulose filter, and analyzed for CD147 by Western blot analysis with rabbit anti-CD147 antibody (a kind gift from Dr. James Bartles). Domain-specific biotinylation was confirmed by Western blot with antibodies to basolateral and apical markers, E-cadherin and gp114, respectively. Blots were visualized by chemiluminescence (Amersham Pharmacia Biotech, Piscataway, NJ). Bands were scanned and intensity was determined using Scion image software (Scion Corporation, Frederick, MD). Biotinylation was performed on each stable clone at least three times. A representative blot is shown in each case.

Domain-specific Cell Surface Biotinylation for Protein-targeting Assay and the Half-life Determination

We performed the targeting assay on the stable clones in MDCK cells overexpressing either CD147 (WT)-GFP or CD147 (L252A)-GFP essentially as described before (Marmorstein *et al.*, 1998b). We utilized C-terminal GFP-tagged CD147 for the assay, because RET-PE2 (against rat CD147) mAb was not a very robust immunoprecipitating antibody. We used rabbit anti-GFP antibody (Abcam, Cambridge, United Kingdom) for immunoprecipitation. This antibody was highly specific and gave no nonspecific signal in nontransfected MDCK cells. Confluent MDCK stable clones were grown on 2.4-cm Transwell filters for 5 days after plating at a density of 1×10^6 cells per filter. Cells were incubated for 40 min in starving medium (DMEM minus methionine and cysteine, 0.2% BSA, and 20 mM HEPES) and pulsed for 30 min (for targeting assay) or 4 h for half-life determination) with [^{35}S]methionine/cysteine (1 mCi ml^{-1} in starving medium; Perkin Elmer-Cetus) applied to the basolateral membranes. A 4-h pulse was performed in starving medium containing 1/10th the concentration of methionine/cysteine of regular medium. Cells were then washed with PBS/CM and kept in chase medium (DMEM, 2.5× Met/Cys and 10% FBS) at 37°C for various times. At the end of each chase time point, the chase medium was removed and the cells were cooled immediately on ice in a cold-room kept at 4°C. Cells were washed four times in ice-cold PBS/CM containing 0.2% BSA. Domain-specific biotinylation was performed as described above. The filters were cut out, frozen at −80°C and lysed the next day in 1 ml lysis buffer (1% Triton X-100, 150 mM sodium chloride, 1 mM EDTA, 0.2% BSA, and 20 mM Tris-HCl at pH 7.4) for 30 min at 4°C. Cell lysates were centrifuged at 28,000 × *g* for 15 min at 4°C to sediment the nuclei. Postnuclear supernatants were collected for immunoprecipitation, which was performed with rabbit anti-GFP antibody and protein A beads (Pierce) overnight at 4°C. The immunoprecipitates were washed as described (Marmorstein *et al.*, 1998b) and nine-tenths of the eluted samples were subsequently reprecipitated with streptavidin-agarose. One-tenth of the eluted immunoprecipitate was used to measure total radioactive incorporation. The samples were analyzed by 12% SDS–PAGE. ^{35}S-labeled proteins were detected using uncoated phosphorscreens and analyzed on a STORM 860 Phosphorimager (Amersham, Piscataway, NJ). Data were quantified by Imagequant version 1.2 (Amersham). The values obtained for the surface biotinylated CD147 were normalized with the total immunoprecipitated CD147 to control for the differential labeling of the filters.

Statistical Analysis

The graphical domain-specific distribution of different CD147 constructs was expressed as mean value ± SD (n ≥ 3).

RESULTS

CD147 Exhibits Reversed Polarity in RPE Compared with Extraocular Epithelial Cells

In our previous work, CD147 was localized to the apical microvilli in the adult rat RPE in vivo in contrast to its basolateral localization in rat kidney tubules and hepatocytes (Marmorstein *et al.*, 1996, 1998a; Finnemann *et al.*, 1997). Here, we have used two well-characterized RPE cell cultures, human fetal RPE and ARPE-19, to localize CD147. As seen in Figure 1, endogenous CD147 is localized apically in both polarized RPE cultures compared with its basolateral localization in extraocular thyroid epithelial (FRT) cells, reiterating our previous observation that CD147 exhibits reversed polarity in RPE.

The Basolateral Signal of CD147 Consists of a Single Leucine in the Cytoplasmic Tail

To unravel the molecular mechanisms behind the reversed polarity of CD147 in RPE, our aim was to identify the basolateral targeting domain of CD147. Because our previous studies implicated the cytoplasmic tail of CD147 in basolateral targeting (Marmorstein *et al.*, 1998a), we generated various truncations, deletions, and point mutations in this region of CD147 and expressed them in a well-characterized prototypic epithelial MDCK cell line (Figure 2). We analyzed the steady state polarity of each construct using laser scanning confocal microscopy and domain-specific biotinylation. We did not find any notable difference in the level of surface expression of the CD147 cytoplasmic constructs used in this study. As shown in Figure 3A, CD147 (WT) is basolaterally targeted in polarized MDCK cells. Steady state biotinylation reveals that >70% of CD147 localizes basolaterally (Figure 3, B and C). Using a biotin assay for endocytosis (Graeve *et al.*, 1989; Marmorstein *et al.*, 1998b), we determined that CD147 does not enter the endocytic pathway (unpublished data).

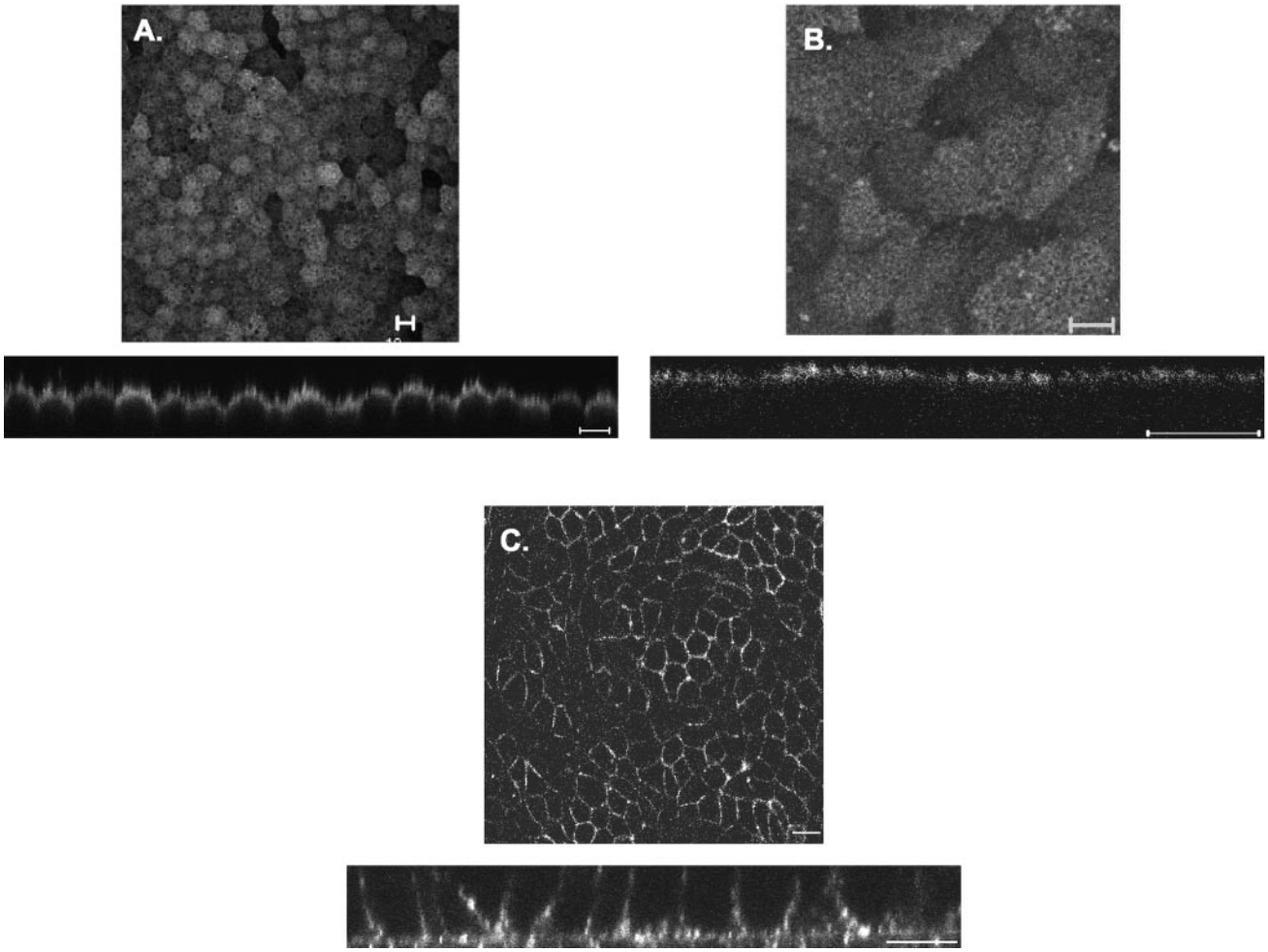

Figure 1. CD147 is apical in RPE and basolateral in FRT cells. Localization of CD147 was performed by indirect immunofluorescence labeling and confocal imaging. Staining was performed with antibody to human CD147 in human fetal RPE (A) and ARPE-19 cells (B) and with anti-RET-PE2 antibody in FRT cells (C). Bar, 10 μm.

To map the basolateral signal in the cytoplasmic tail of CD147, we progressively truncated stretches of 11 amino acids from the cytoplasmic tail of CD147. As seen in Figure 3A, CD147 (262) devoid of its C-terminal 11 amino acids had a steady state distribution similar to that of the wild-type protein (Figure 3, B and C). In contrast, a 21-amino acid truncation of the cytoplasmic tail resulted in mistargeting of CD147 (252) to the apical domain (Figure 3). In stable MDCK clones, the steady state distribution of CD147 (252) was 80% apical (Figure 3B and 3C). This suggested that CD147 harbors a basolateral targeting signal between the 11th and 21st amino acid from the C-terminal end, i.e., between amino acids 252 and 262. Not surprisingly, CD147 (242) with a 30-amino acid C-terminal truncation was also targeted apically (Figure 3).

To further dissect the region encoding the putative basolateral signal, we next engineered internal deletions of four amino acids within the target signal region of amino acids 252–262, as shown in Figure 2. CD147 mutants with deletion of amino acids 259–263 or 256–259 were sorted basolaterally (Figure 4, A–C). In contrast, deletion of amino acids 252–255 resulted in apical reversal of the polarity of CD147 (Figure 4A). Almost 80% of this CD147 mutant was mistargeted apically (Figure 4, B and C). The above observations were made independently by confocal microscopic analysis and domain-specific biotinylation. Because amino acids 252–255 were found to be critical in basolateral sorting, our further studies focused on analyzing the role of these amino acids individually. Cytoplasmic tail amino acids 252–255 of CD147 are leucine, lysine, glycine, and serine. We point-mutated these four amino acids individually to alanine (Figures 5 and 6). Interestingly, mutating the hydrophobic leucine to alanine (L252A) completely reversed the trafficking of CD147. As seen in Figure 6, this leucine seems to be a key component of the basolateral signal as 80% of CD147 (L252A) was localized to the apical domain. Point mutation of lysine (253), glycine (254), and serine (255) to alanine did not have any effect on basolateral targeting of CD147 (Figure 5). A single leucine motif has been identified as the basolateral determinant in only one other protein, stem cell factor (SCF; Wehrle-Haller and Imhof, 2001)

The Presence but not the Charge of Amino Acids at Position 243–246 Is Essential for Basolateral Targeting of CD147

The cluster of acidic amino acids residing N-terminal to leucine 263 is critical for efficient basolateral targeting of stem cell factor. Substitution of this acidic cluster to alanines resulted in nonpolarized trafficking of stem cell factor (Wehrle-

Cytoplasmic Tail of CD147	Construct Name	Deletion	Polarity
NH_2-Terminal COOH-terminal			
232 aa 272aa			
YEKRRKPDQT LDEDDPGAAP LKGSGSHLND KDKNVRQRNAT	wild-type	----------	BL
YEKRRKPDQT LDEDDPGAAP LKGSGSHLND	262	11 amino acids	BL
YEKRRKPDQT LDEDDPGAAP	252	21 amino acids	AP
YEKRRKPDQT	242	31 amino acids	AP
YEKRRKPDQT LDEDDPGAAP .....GSHLND KDKNVRQRNAT	d252-255	4 amino acids	AP
YEKRRKPDQT LDEDDPGAAP LKGS.....ND KDKNVRQRNAT	d256-259	4 amino acids	BL
YEKRRKPDQT LDEDDPGAAP LKGSGSHL..... .... KNVRQRNAT	d259-263	4 amino acids	BL
YEKRRKPDQT LDEDDPGAAP **A**KGSGSHLND KDKNVRQRNAT	L252A	Substitution	AP
YEKRRKPDQT LDEDDPGAAP L**A**GSGSHLND KDKNVRQRNAT	K253A	Substitution	BL
YEKRRKPDQT LDEDDPGAAP LK**A**SGSHLND KDKNVRQRNAT	G254A	Substitution	BL
YEKRRKPDQT LDEDDPGAAP LKG**A**GSHLND KDKNVRQRNAT	S255A	Substitution	BL
YEKRRKPDQT **A**DEDDPGAAP LKGSGSHLND KDKNVRQRNAT	L242A	Substitution	BL
YEKRRKPDQT LDEDDPGAAP LKGSGSH**A**ND KDKNVRQRNAT	L259A	Substitution	BL
YEKRRKPDQT LDEDDPGAA**A** LKGSGSHLND KDKNVRQRNAT	P251A	Substitution	BL
YEKRRKPDQT L.....PGAAP LKGSGSHLND KDKNVRQRNAT	d243-246	4 amino acids	AP
YEKRRKPDQT L**AAAA**PGAAP LKGSGSHLND KDKNVRQRNAT	243-246A	Substitution	BL
YEKRRKPDQT LDEDDP..... LKGSGSHLND KDKNVRQRNAT	d248-251	4 amino acids	NP
YEKRRKPDQ**A** LDEDDGAAP LKGSGSHLND KDKNVRQRNAT	T241A	Substitution	BL
YEKRRKPDQT LDEDDPGAAP **I**KGSGSHLND KDKNVRQRNAT	L252I	Substitution	BL

Figure 2. A schematic representation of different cytoplasmic domain constructs of CD147 utilized in this study. A dotted line suggests deleted amino acids and bold and underlined amino acid represents substitution by point mutation. BL, basolateral; AP, apical; NP, nonpolar.

Haller and Imhof, 2001). Moreover, an acidic cluster near the di-hydrophobic motif (FI) is a basolateral targeting signal in furin protease (Simmen *et al.,* 1999). CD147 has a cluster of acidic amino acids N-terminal to leucine 252. To determine the role of this acidic cluster in CD147 localization, we initially deleted amino acids 243–246 (DEDD). This deletion triggered mistargeting of CD147 to the apical domain (Figure 6). Intriguingly, substitution of this acidic cluster with four alanine residues (243–246A) did not affect the basolateral targeting of CD147 (Figure 7), suggesting that the presence of four residues, irrespective of their identity and polar side-chain, are sufficient for basolateral targeting, if leucine 252 is present. Probably, some critical amino acids N-terminal to these four residues (243–246) might have an accessory role in the basolateral targeting of CD147. Thus, the residues 243–246 may maintain appropriate spacing between leucine 252 and these putative critical residues needed for recognition by basolateral sorting machinery. Additionally, upon deletion of four amino acids (248–251) that separate leucine 252 from amino acids 243–246, the distribution of CD147 was found to be nonpolar. The equal distribution of CD147 (248–251) between apical and basolateral domains suggests that the preservation of the length of the region between leucine 252 and amino acids N-terminal to it is essential for efficient targeting of CD147 (Figure 7).

Determining the Role of Other Single Leucines and of Amino Acids Juxtaposed to Leucine 252 in Basolateral Trafficking of CD147

Altering any hydrophobic leucine could modulate the secondary and the tertiary structure of the cytoplasmic tail of CD147. This may affect the recruitment of CD147 in vesicles en route to the basolateral membrane. To address this possibility, we point-mutated two other leucine residues from the cytoplasmic tail of CD147. As seen in Figure 8, CD147 (L242A) and CD147 (L259A) were both targeted basolaterally. Thus, leucines 242 and 259 do not play a role in determining the basolateral targeting of CD147. In addition to tyrosine and di-leucine motifs, basolateral targeting signals may include di-hydrophobic motifs, such as *FI* for furin (Simmen *et al.,* 1999), *LV* for CD44 (Sheikh and Isacke, 1996), or *LI* and *ML* for invariant chains (Odorizzi and Trowbridge, 1997; Simonsen *et al.,* 1997). In CD147, a di-hydrophobic motif could result from proline 251 next to leucine 252 (although proline's hydrophobicity is considerably lower than that of leucine, isoleucine, phenylalanine, methionine, and valine). Nonetheless, mutation of proline 251 to alanine in CD147 (P251A) resulted in faithful basolateral targeting, further confirming that the basolateral signal resides only in leucine 252 (Figure 8).

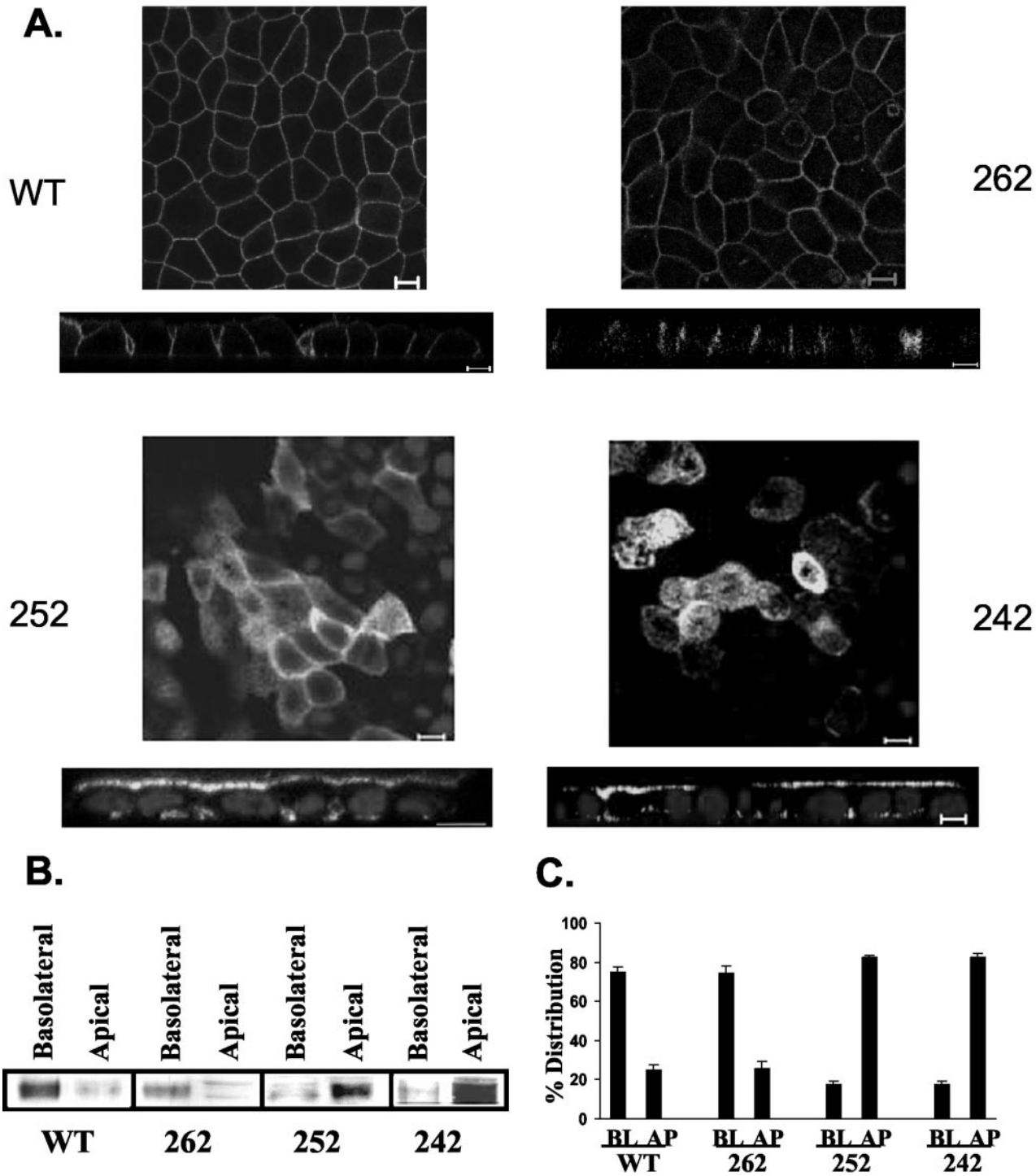

Figure 3. Basolateral signal of CD147 resides between 11–21 amino acids from the C-terminal. (A) Confocal images (*xy* and *xz* view) obtained by staining with anti-RET-PE2 antibody. An individual *xy* section is shown. MDCK cells overexpressing CD147 (252 and 262) are also stained for nuclei with TO-PRO-3 iodide. (B) Steady state polarity was determined by domain-selective biotinylation. Biotinylated proteins were captured by streptavidin-agarose and Western blotting was performed with rabbit anti-CD147 antibody. A 50-kDa band of CD147 was observed. (C) Quantification of distribution between basolateral (BL) and apical (AP) domains (n = 3) of wild-type and different cytoplasmic mutants of CD147 stably expressed in MDCK cells. Bar, 10 μm.

The Basolateral Signal of CD147 Is Transplantable to Other Proteins

The extracellular domain of a CD147 could aid in trafficking of the protein by dimerization or by association with other proteins (Yoshida *et al.,* 2000). To determine whether the extracellular domain of CD147 has any independent trafficking function, we fused the transmembrane and cytosolic domains of CD147 with the extracellular domain of Tac, the

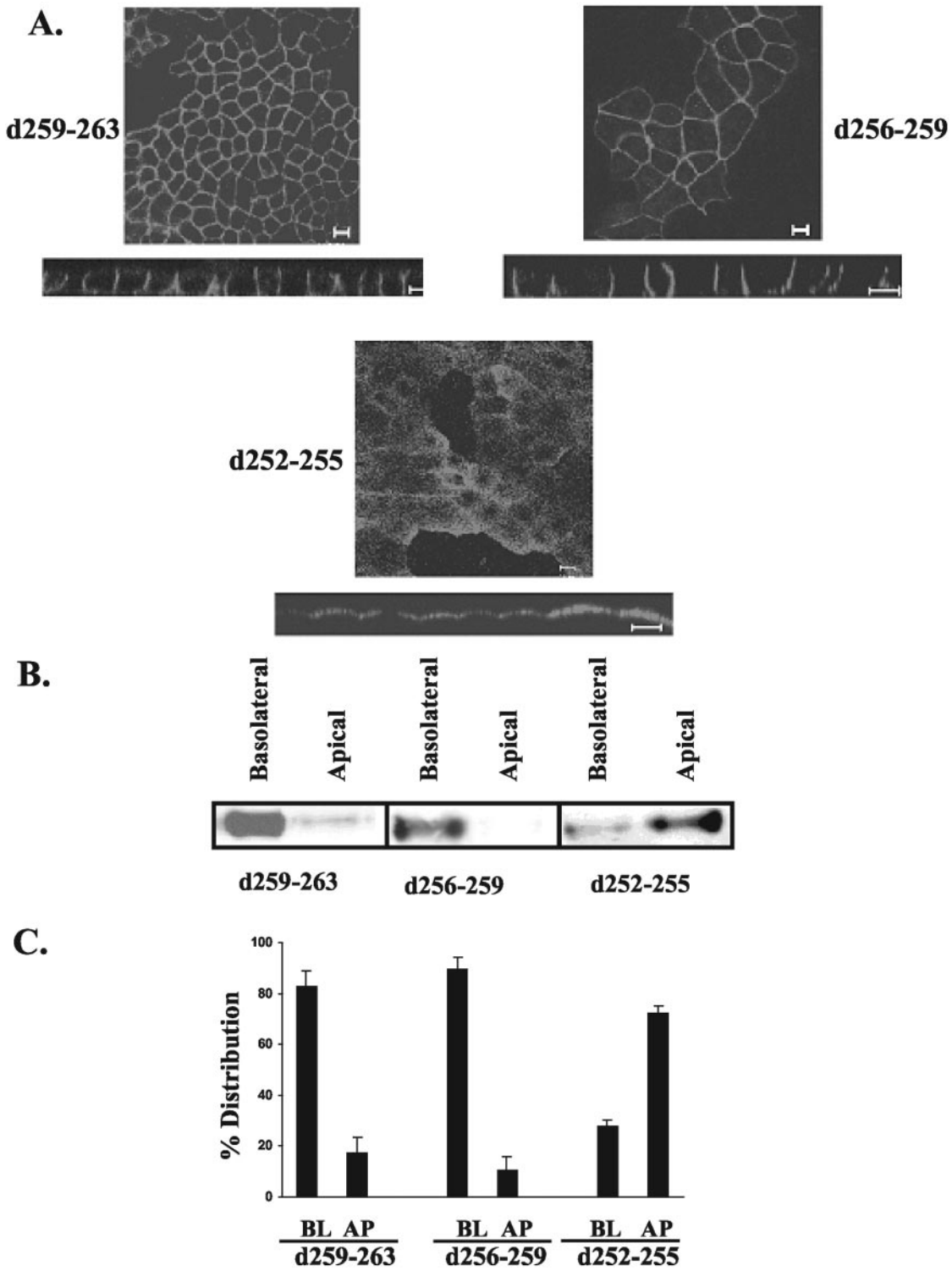

Figure 4. Basolateral signal of CD147 lies between amino acids 251–254. MDCK cells stably expressing different CD147 constructs with four amino acid deletions were subjected to immunofluorescence and domain-specific biotinylation (A) Confocal images (single *xy* section and *xz* view) obtained by staining MDCK cells with anti-RET-PE2 antibody. (B) Steady state distribution of various CD147 mutants by cell surface biotinylation and detection of biotinylated CD147 by Western blotting with rabbit anti-CD147 antibody. (C) Quantification of the percentage distribution of CD147 mutants between basolateral (BL) and apical (AP) domains (n = 3). Bar, 10 μm.

interleukin-2 receptor alpha chain. Full-length Tac is targeted apically in MDCK cells (Figure 9A). In contrast, the Tac-CD147 (WT) chimera was delivered basolaterally (Figure 9B). Abrogating the leucine signal in Tac-CD147 (L252A) or deleting the acidic amino acid cluster Tac-CD147 (d243–246) from the cytoplasmic tail of the Tac-CD147 chimera

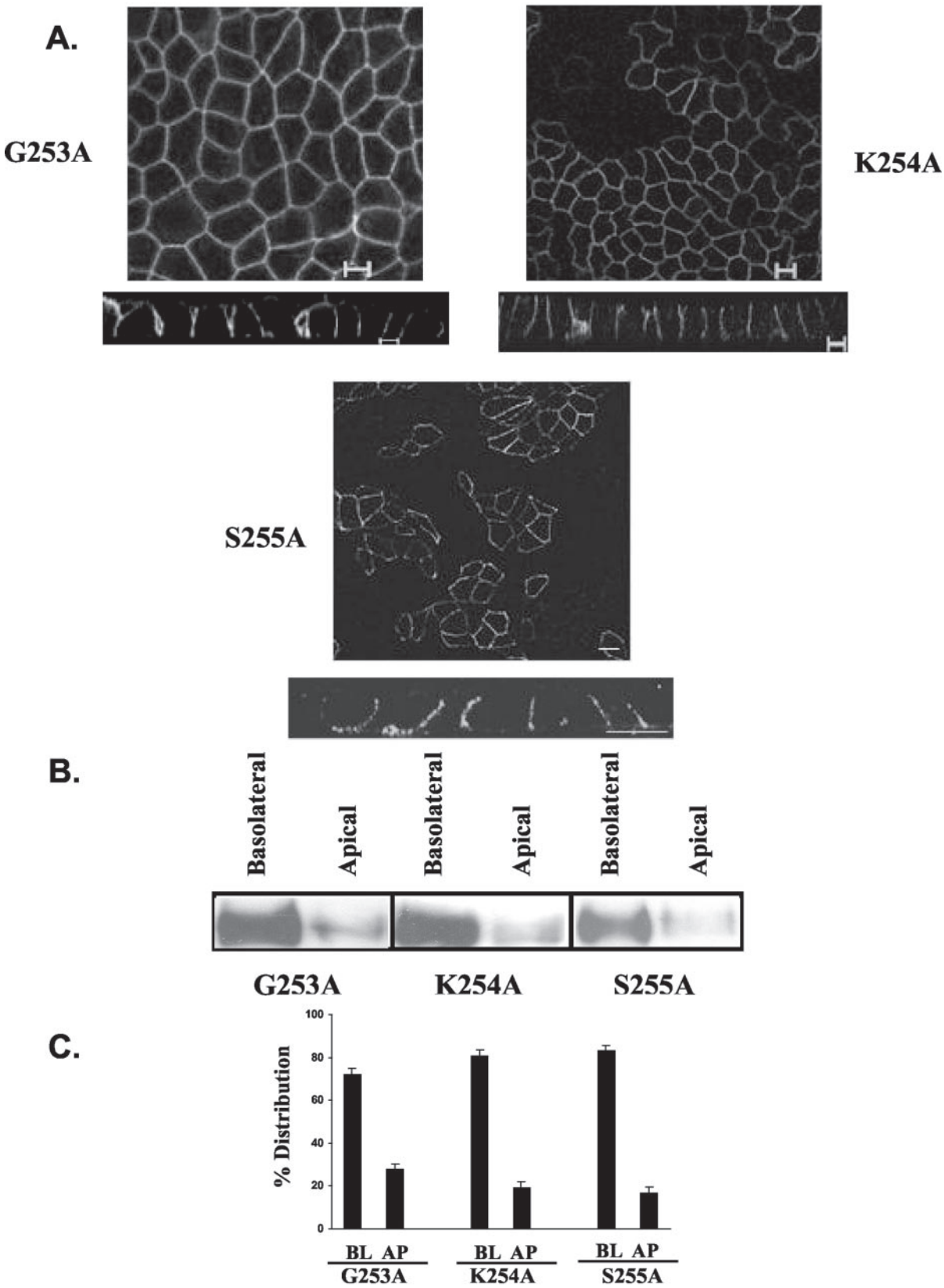

Figure 5. Amino acids 253–255 are not involved in basolateral trafficking of CD147. The horizontal (*xy*) and vertical (*xz*) confocal images of MDCK stable clones expressing CD147 constructs and stained with anti-RET-PE2 antibody (A) along with domain-specific biotinylation and Western blotting for CD147 (B) and the quantification of the polarized distribution (C) show basolateral localization of all the three constructs of CD147 harboring point mutations. BL, basolateral; AP, apical. Bar, 10 μm.

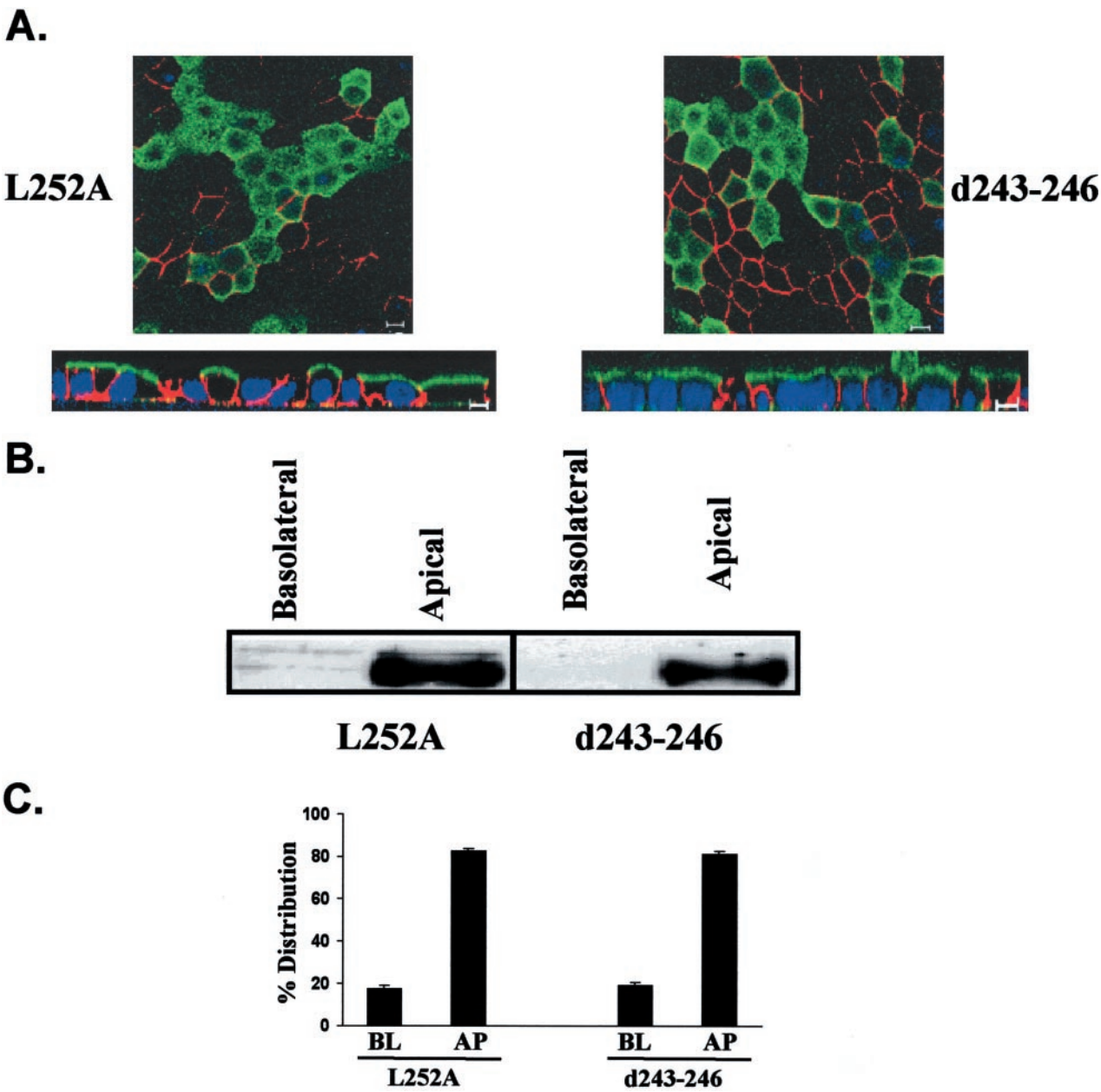

Figure 6. Leucine (252) and amino acid cluster (243–246) are both essential for basolateral targeting of CD147. Independent analysis by immunofluorescence staining with anti-RET-PE2 antibody and confocal imaging (single *xy* section and *xz* view) (A) and domain-specific biotinylation and detection of CD147 by Western blot analysis (B) show that by mutating leucine (252) and deleting amino acid cluster 243–246, CD147 exhibits reversed polarity and is targeted to the apical domain. On quantification, an average of 80% of the steady state protein was found to reside in the apical membrane (n = 3) (C). In A, β-catenin (red) represents the lateral staining. Nuclei are stained with TO-PRO-3 iodide (blue) and CD147 (green) was stained with anti–RET-PE2 antibody. BL, basolateral; AP, apical. Bar, 10 μm.

perturbs the basolateral targeting because both chimeric proteins are localized in the apical domain (Figure 9C and 9D). Thus, the cytoplasmic domain of CD147 acts as a transplantable basolateral signal.

CD147(WT) and CD147(L252A) Are Targeted Directly to Their Site of Steady State Accumulation and Have Similar Half-lives

To obtain more insight into the events that lead to different steady state localizations of CD147(WT) and CD147(L252A), we studied their biosynthetic targeting by pulse-chase analysis and domain-specific surface biotinylation. The assay was performed in stable MDCK clones expressing similar levels of GFP-tagged CD147(WT) or GFP-CD147(L252A). The GFP tag at the C-terminus did not affect the targeting of the molecules (see Supplementary Material). GFP-tagged CD147 was used for this assay because of lack of robust immunoprecipitating antibody against rat CD147. As seen in Figure 10A, CD147(WT)-GFP was directly targeted to the basolateral membrane. Notably, the CD147(L252A)-GFP mutant was also directly delivered to its steady state apical localization. Moreover, the L252A mutation did not affect the half-life of CD147 (Figure 10B). The half-lives of CD147

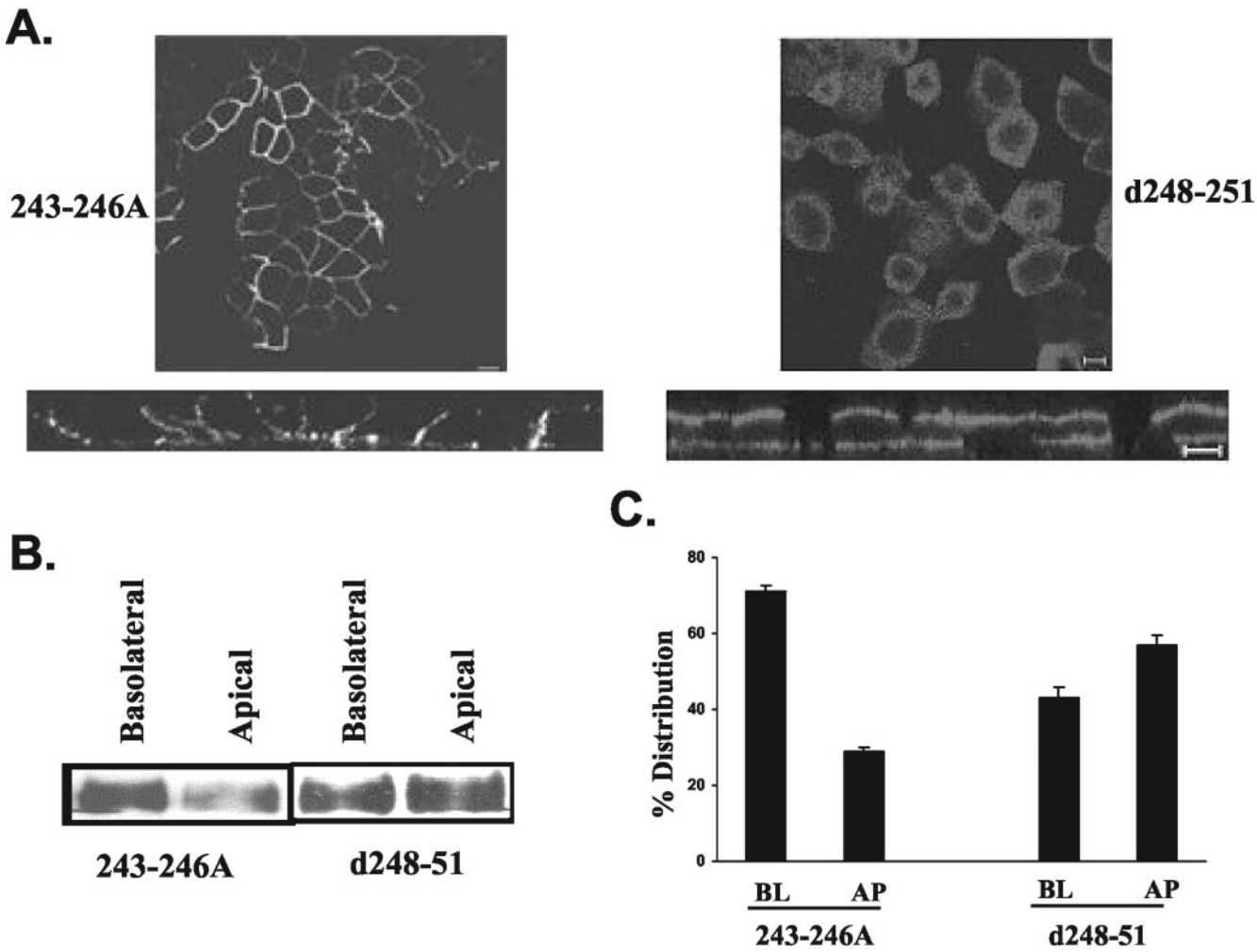

Figure 7. Role of acidic amino cluster 243–246 and amino acid 248–251. Substitution of acidic amino acid cluster with alanines did not affect the basolateral targeting of CD147. Deletion of amino acids 248–251 separating leucine 252 and amino acid 243–246 resulted in nonpolar distribution of CD147. (A) Confocal sections (single *xy* section and *xz* view) obtained by immunostaining with anti–RET-PE2 antibody (B). Cell surface biotinylation and Western blot analysis for CD147 (C). Quantitation of percentage of surface distribution of CD147 in stable MDCK clones expressing these two constructs of CD147. BL, basolateral; AP, apical. Bar, 10 μm.

(WT) and CD147 (L252A) were both ~12–16 h as determined by two independent experiments. In addition, we determined that both proteins have similar half-lives at basolateral and apical membranes (Figure 10B).

CD147 Does Not Utilize Adaptin AP1B for Basolateral Sorting

In the porcine kidney epithelial cell line LLC-PK1 some basolateral membrane proteins like H,K-ATPase, low-density lipoprotein receptor, and transferrin receptor exhibit a defect in targeting, resulting in their appearance at the apical surface (Roush *et al.*, 1998, Folsch *et al.*, 1999; Gan *et al.*, 2002). This defect is due to the absence of the μ1B subunit of the adaptin AP1B in these cells (Ohno *et al.*, 1998; Roush *et al.*, 1998; Folsch *et al.*, 1999). Although AP1B has affinity for a consensus tyrosine motif, it has been shown that the beta-subunit of AP1 can bind to a leucine motif. Alternatively, an accessory protein like PACS-1 might be acting as a piggy-back linker associating CD147 to AP1B (Rapoport *et al.*, 1998; Wan *et al.*, 1998). Moreover, AP1B has been implicated in targeting cargo directly at the biosynthetic pathway as well as in the recycling route (Folsch *et al.*, 1999, 2003; Gan *et al.*, 2002) Thus, we transfected CD147 into LLC-PK1 cells to directly test the involvement of AP1B in its basolateral localization. The stably transfected LLC-PK1 clones exhibited basolateral polarity of CD147 (WT; Figure 11). This finding rules out the involvement of AP1B machinery in recruiting and transporting CD147 to the basolateral domain. The CD147 (L252A) mutant was targeted apically in LLC-PK1 cells (Figure 11). Thus the sorting machinery responsible for basolateral sorting of CD147 is present in both MDCK and LLC-PK1 cells and recognizes L252. GGAs are known to sort proteins with an acidic cluster–di-leucine motif from Golgi to the endosomal system (Puertollano *et al.*, 2001). To determine any interaction of the leucine-based signal of CD147 with GGAs, we performed yeast two-hybrid screening of the interaction between the cargo-binding VHS domain of GGAs1–3 and the cytoplasmic domain of CD147. We detected no direct interaction of CD147's cytoplasmic tail with the VHS domain of the adaptins GGA1–3 (unpublished data).

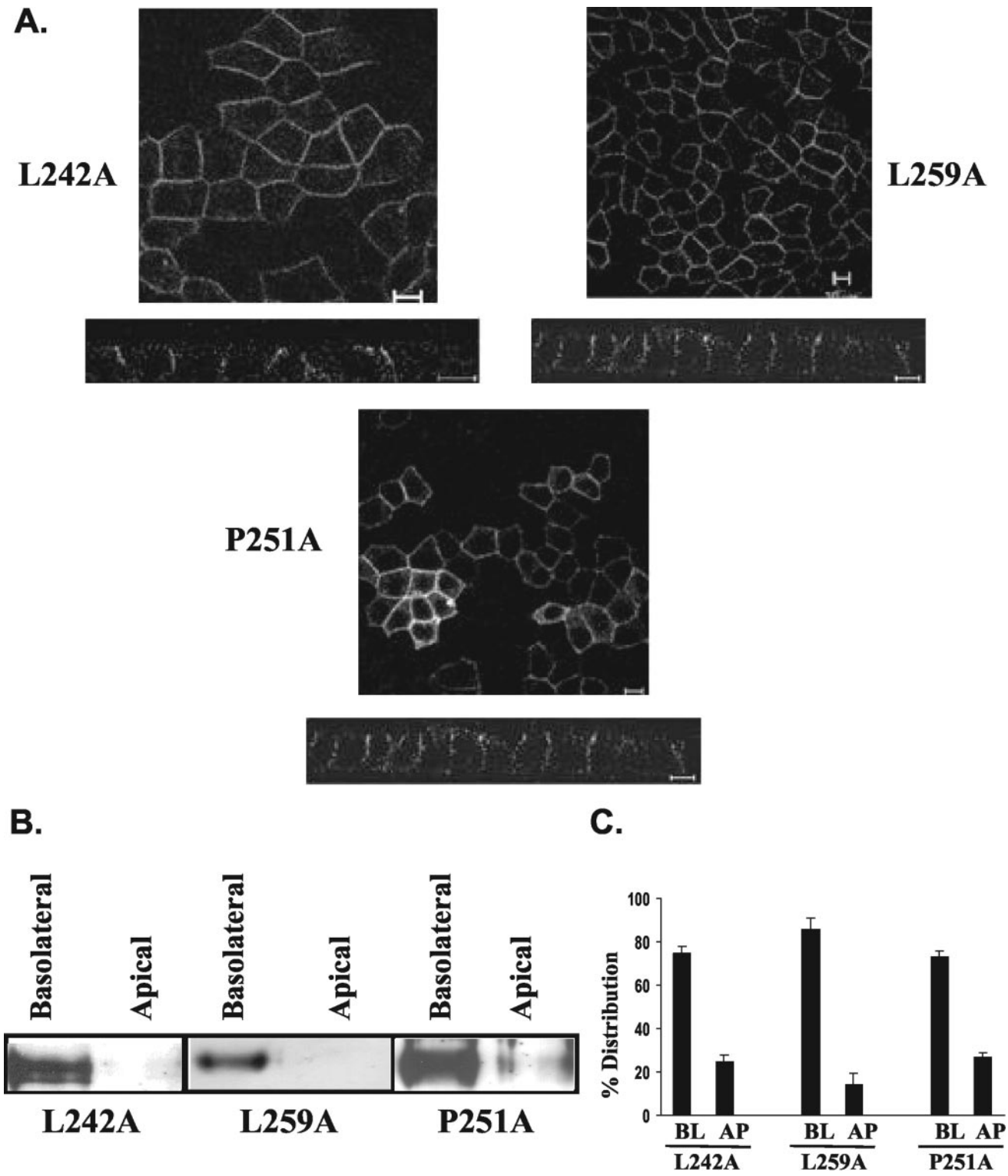

Figure 8. Only leucine 252 is involved in basolateral targeting of CD147. Mutating leucine 242 and leucine 259 to alanine, basolateral targeting of CD147 is not affected. Proline 251, adjacent to leucine 252, does not influence the targeting of CD147. Inference was drawn by performing immunostaining with anti–RET-PE2 antibody and confocal analysis (A) and steady state domain-specific biotinylation of the above constructs and detection of biotinylated CD147 by Western blot analysis (B). The distribution of surface biotinylated protein was performed to determine domain-specific distribution of CD147 stable clones obtained from transfecting above constructs (C). BL, basolateral; AP, apical. Bar, 10 μm.

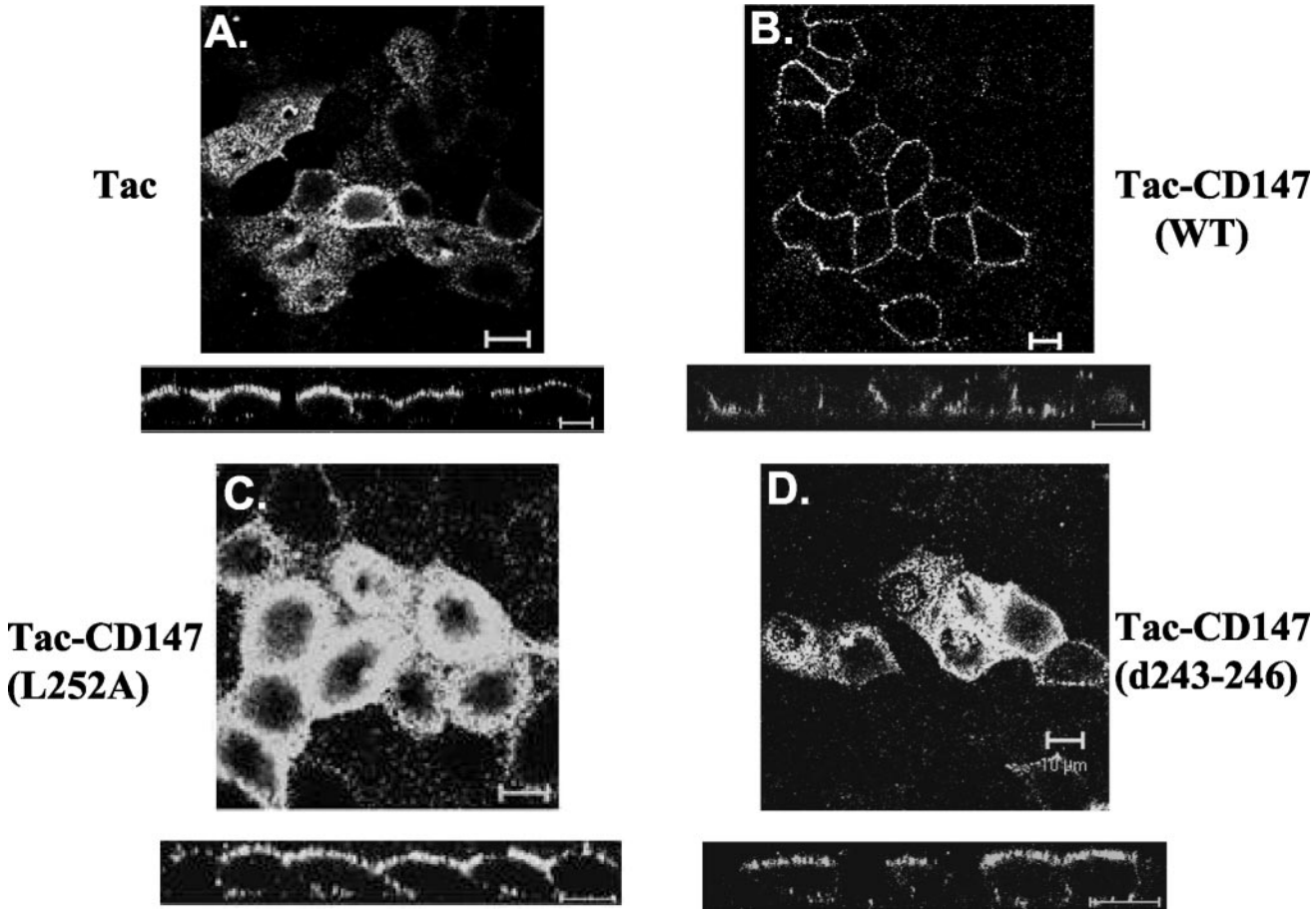

Figure 9. Basolateral signal of CD147 is transplantable to other proteins. The confocal images (individual *xy* section and *xz* view) show that full-length Tac is targeted to the apical membrane (A), whereas Tac-CD147 (WT) chimera is rerouted to the basolateral membrane (B). The basolateral targeting of the chimera was abrogated by point mutating leucine 252 to alanine in Tac-CD147 (L252A) (C) and deleting acidic cluster Tac-CD147 (243–246) (D), emphasizing the role of these two motifs present in the cytoplasmic domain of CD147 in determining basolateral membrane delivery. Immunostaining was performed with anti-Tac antibody. Bar, 10 μm.

ARPE-19 Cells Do Not Recognize the Basolateral Sorting Signal of CD147

ARPE-19 is a spontaneously derived human RPE cell line that retains various characteristics of RPE in situ (Dunn *et al.*, 1996). ARPE-19 cells were polarized for 6 weeks on laminin-coated Transwell filters. We transfected both the polarized ARPE-19 cells and polarized MDCK cells with cDNAs of CD147(WT)-GFP, CD147 (L252A)-GFP, Tac-CD147 (WT), and Tac-CD147 (L252A). Unlike polarized MDCK cells, ARPE-19 cells failed to recognize the basolateral signal of CD147 and did not distinguish the CD147 with or without leucine 252. As seen in Figure 12, the wild-type as well as leucine mutant of CD147 are targeted apically along with endogenous human CD147. As expected, MDCK cells discriminated between these two constructs and targeted CD147 (WT) to the basolateral membrane and CD147 (L252A) to the apical membrane. An alternative interpretation of these results is that RPE cells might "read" a cryptic apical signal present in the ectodomain of CD147 that is dominant over the cytoplasmic basolateral signal, resulting in the observed apical sorting of CD147 in RPE. To address this issue, we transfected ARPE-19 cells with a chimera of the ectodomain of the Tac and the transmembrane and cytoplasmic domains of wild-type or L252A CD147 (Tac-CD147). We found the Tac-CD147 chimera was targeted apically in ARPE-19 cells (Figure 12) and the Tac-CD147(L252A) chimera was targeted apically both in MDCK and ARPE-19 cells (unpublished data). These experiments support the idea that the basolateral signal in the cytoplasmic domain of CD147 is not recognized by RPE.

Finally, we tested the sorting of the other protein known to have a monoleucine basolateral signal, SCF. SCF-GFP was mainly cytoplasmic in ARPE-19 cells; however, a few ARPE cells targeted it apically. MDCK targeted SCF-GFP to the basolateral membrane (Figure 12; Wehrle-Haller and Imhof, 2001).

DISCUSSION

The striking reversed polarity of CD147 in RPE cells elicited our interest in understanding the sorting signals in this protein. Because the cytoplasmic domain of CD147 is devoid of well-characterized basolateral signals, such as tyrosine and di-leucine motifs, we undertook a systematic approach to localize basolateral targeting information in CD147. Our detailed analysis identified a single leucine as the basolateral targeting motif of CD147. This type of basolateral signal has been described in only one other protein, the stem cell factor (Wehrle-Haller and Imhof, 2001). The importance of leucine 252 in the biology of CD147 is underscored by its conserva-

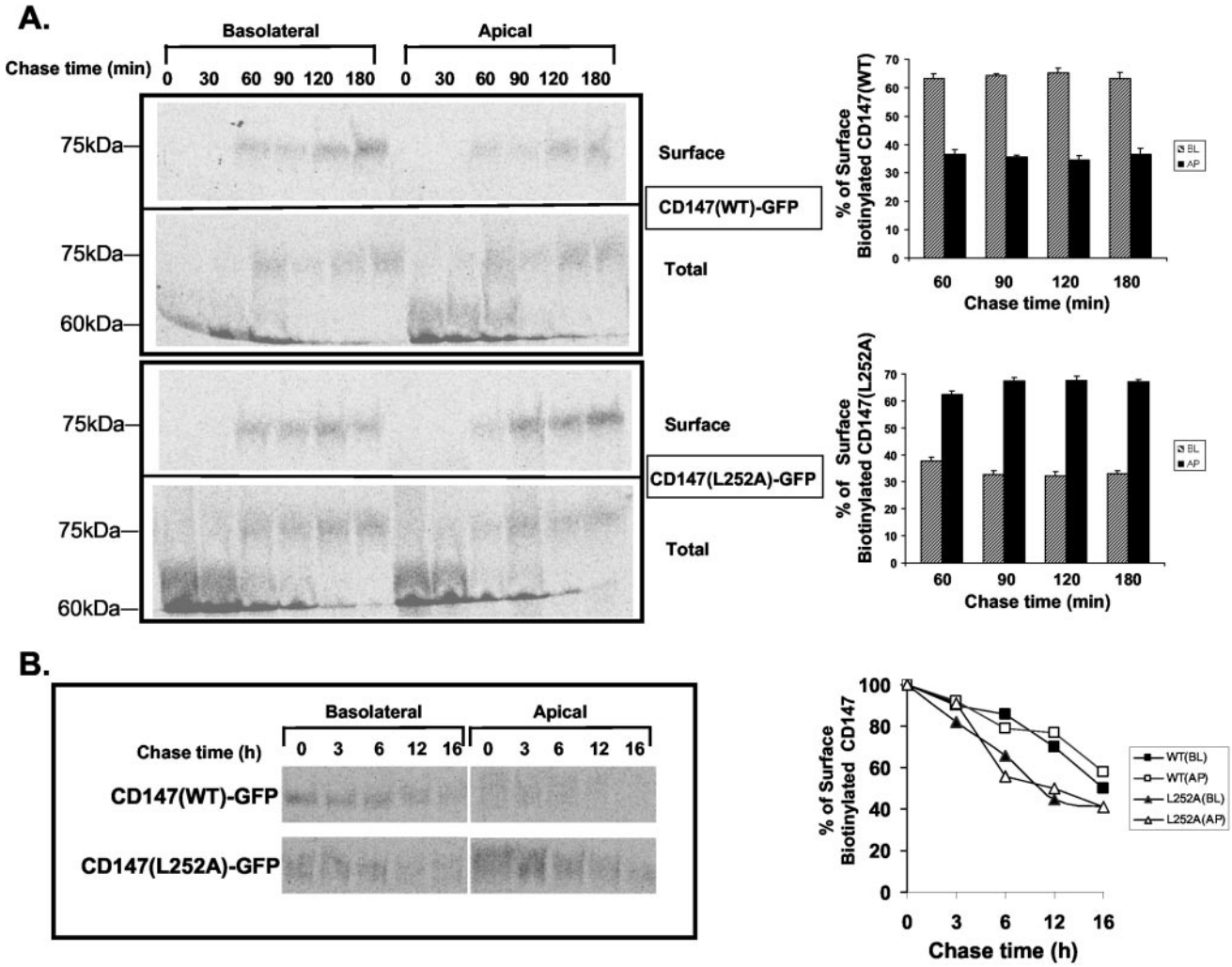

Figure 10. Direct delivery of CD147 (WT) and CD147 (L252A) to steady state membrane domains and L252A mutation and the stability of CD147. (A) Targeting assay followed by domain selective biotinylation in MDCK stable clones overexpressing CD147 (WT)-GFP and CD147 (L252A)-GFP imply that both the proteins are targeted directly to their site of steady state accumulation. Percentage of surface biotinylated CD147 was calculated by normalizing with total (immature form at 60-kDa and mature form at 75 kDa) immunoprecipitated CD147. The graphical representation of polarized distribution of CD147 (WT)-GFP and CD147 (L252A)-GFP represents the average of five independent experiments. (B) Stability of CD147 (WT)-GFP and CD147 (L252A)-GFP was similar as assessed by chasing the proteins for 16 h. Both the proteins have similar half-lives at the apical and the basolateral membranes. Results are from two independent experiments.

tion in human, mouse, rat, chicken, hamster, and zebrafish (Figure 13).

The CD147 signal, however, was not identical to the basolateral signal of stem cell factor. Unlike stem cell factor, basolateral targeting of CD147 does not require an acidic amino acid cluster, because replacement of these amino acids by alanines did not result in apical mistargeting. It is likely that in CD147 these residues may not participate in electrostatic interaction with the sorting machinery, but a stretch of four amino acids at the position 243–246 may only be needed to maintain appropriate spacing between leucine 252 and some critical residues N-terminal to these four residues. This is suggested by the observation that deletion of residues 243–246 promote apical targeting of CD147 (Figure 6). In contrast, in stem cell factor, replacing the acidic cluster with alanines results in nonpolar distribution of the protein by immunofluorescence (Wehrle-Haller and Imhof, 2001; no biochemical analysis of polarity was performed in that study). It will be interesting to determine whether the difference in the stringency of the requirement for the acidic cluster reflects interaction with different sorting components or just a flexible interaction with the same sorting machinery. The sorting signal of CD147 shares with the basolateral signal of polymeric IgG the requirement for a single amino acid in basolateral targeting. The basolateral targeting domain of the polymeric IgG receptor includes a mono-valine in a β-turn conformation in addition to three and four amino acids N-terminal to valine (Aroeti *et al.*, 1993). We subjected the cytoplasmic tail of CD147 to β-turn prediction by five different statistical algorithms (Kaur and Raghava, 2002a, 2002b). As deduced by these algorithms, leucine 252 does not have a propensity for acquiring a β-turn conformation, possibly implying that the signal of CD147 is distinct from that of polymeric IgG receptor.

Various cytoplasmic constructs of CD147 gave us interesting insights on the structural requirements of CD147's basolateral determinant. Deletion of four amino acids (248–251) between leucine 252 and amino acids 243–246 prevents

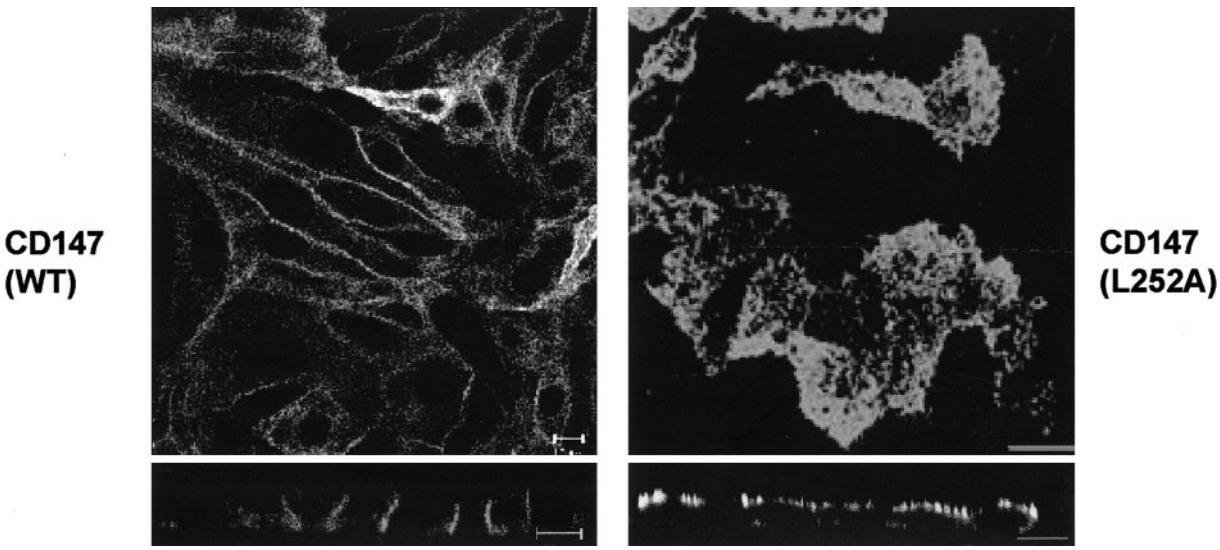

Figure 11. Trafficking of CD147 is not mediated by adaptin AP1B. LLC-PK1 cells lacking the adaptin AP1B were transfected with CD147 (WT) and CD147 (L252A) cDNA. Filter grown stable clones obtained were analyzed for localization of CD147 by immunofluorescence with anti–RET-PE2 antibody. The confocal individual xy section and xz view images show basolateral and apical distribution of CD147 (WT) and L252A mutant, respectively. Bar, 10 μm.

efficient targeting of CD147 (Figure 7). Probably, because of change in the spacing and the structural alterations imposed by deleting these four amino acids (248–251) the sorting machinery may be binding to leucine 252 of this mutant less efficiently, leading to nonpolar distribution of this CD147 mutant.

Modulating the hydrophobicity of the protein structure by mutating leucine to alanine would affect the secondary and tertiary structure of the protein. This may in turn affect its trafficking properties in a nonspecific manner. We addressed this issue by mutating two other leucine residues (242 and 259) along with leucine 252. As seen in Figures 6 and 8, only leucine 252 is crucial for basolateral trafficking of CD147; the other two leucine residues did not alter trafficking of CD147. Moreover, the possible involvement of a di-hydrophobic signal was ruled out, because mutating a proline residue adjacent to leucine 252 did not alter the polarity of CD147 (Figure 8). A CKII phosphorylation motif plays a critical role in sorting of the cation-independent mannose 6-phosphate receptor (Kato *et al.*, 2002). CD147 harbors the putative CKII motif juxtaposed to the critical acidic cluster (TLDEDD). A role for CKII phosphorylation in sorting was ruled out, because mutating a threonine residue (T241A) within this domain did not affect the basolateral transport (unpublished data). A conservative substitution of leucine 252 to isoleucine did not affect the basolateral targeting of CD147 (see Supplementary Material).

We performed targeting assays to determine the delivery route of CD147 (WT) and CD147 (L252A) to their respective steady state membrane domains. Our results suggest that both the WT and the L252A mutant are delivered directly to the basolateral and apical membrane, respectively (Figure 10A). This observation indicates that CD147 (WT) or L252A mutant do not utilize a transcytotic route in MDCK cells. Perturbing the basolateral motif in the L252A mutant may unmask a recessive cryptic apical signal that may direct targeting to the apical membrane. The L252 mutation did not affect the stability of the protein, because its half-life was similar to the CD147 (WT) (Figure 10B).

We made an attempt to identify an adaptin involved in trafficking of CD147. CD147 was expressed in LLC-PK1 cells, known to lack the μ1B subunit (Ohno *et al.*, 1998; Roush *et al.*, 1998; Folsch *et al.*, 1999). Absence of this subunit did not affect the basolateral trafficking of CD147, implying the involvement of adaptins other than AP1B (Figure 9). We performed yeast two-hybrid screening of the cytoplasmic tail of CD147 with the VHS-domain of the monomeric adaptors GGA 1–3 known to bind cargo with acidic cluster–di-leucine motifs (Puertollano *et al.*, 2001). We observed no interaction in our in vitro analysis (unpublished data). In our future studies involving different APs, we will utilize the new technique of yeast three-hybrid assay, which attempts to recapitulate in situ interactions involving hemicomplexes of AP adaptors (Janvier *et al.*, 2003). In this in vitro assay, two subunits of the AP complex were used to determine the interaction with di-leucine–based sorting signal. We shall extend our interaction studies in the future to include various non-AP adaptors such as epsin, STAM, and Hrs (Bonifacino and Traub, 2003). An additional probability is that sorting of CD147 does not involve cognate adaptors and is mediated by direct interaction with a motor, as shown for rhodopsin (Tai *et al.*, 1999). Identification of AP- or non-AP–based sorting machinery for CD147 and detailed structural analysis of its interaction with leucine 252 of CD147 should provide insights on the mechanisms of recognition and specificity achieved through a single leucine residue.

ARPE-19 cells are a spontaneously immortalized human RPE cell line. These cells are among the best in vitro models for polarity studies of RPE (Dunn *et al.*, 1996, 1998). These cells require ~6 weeks to express differentiation-specific genes including RPE65 and CRALBP (Alizadeh *et al.*, 2001). Moreover, the cells were cultured in Chee's essential replacement medium known to aid RPE cells in differentiation (Hu and Bok, 2001). As seen in Figure 12, our observation confirms that RPE cells do not recognize the basolateral motif of CD147 and unlike polarized MDCK cells, RPE cells cannot distinguish between wild-type and leucine (L252A) mutant. To determine whether silencing of the putative

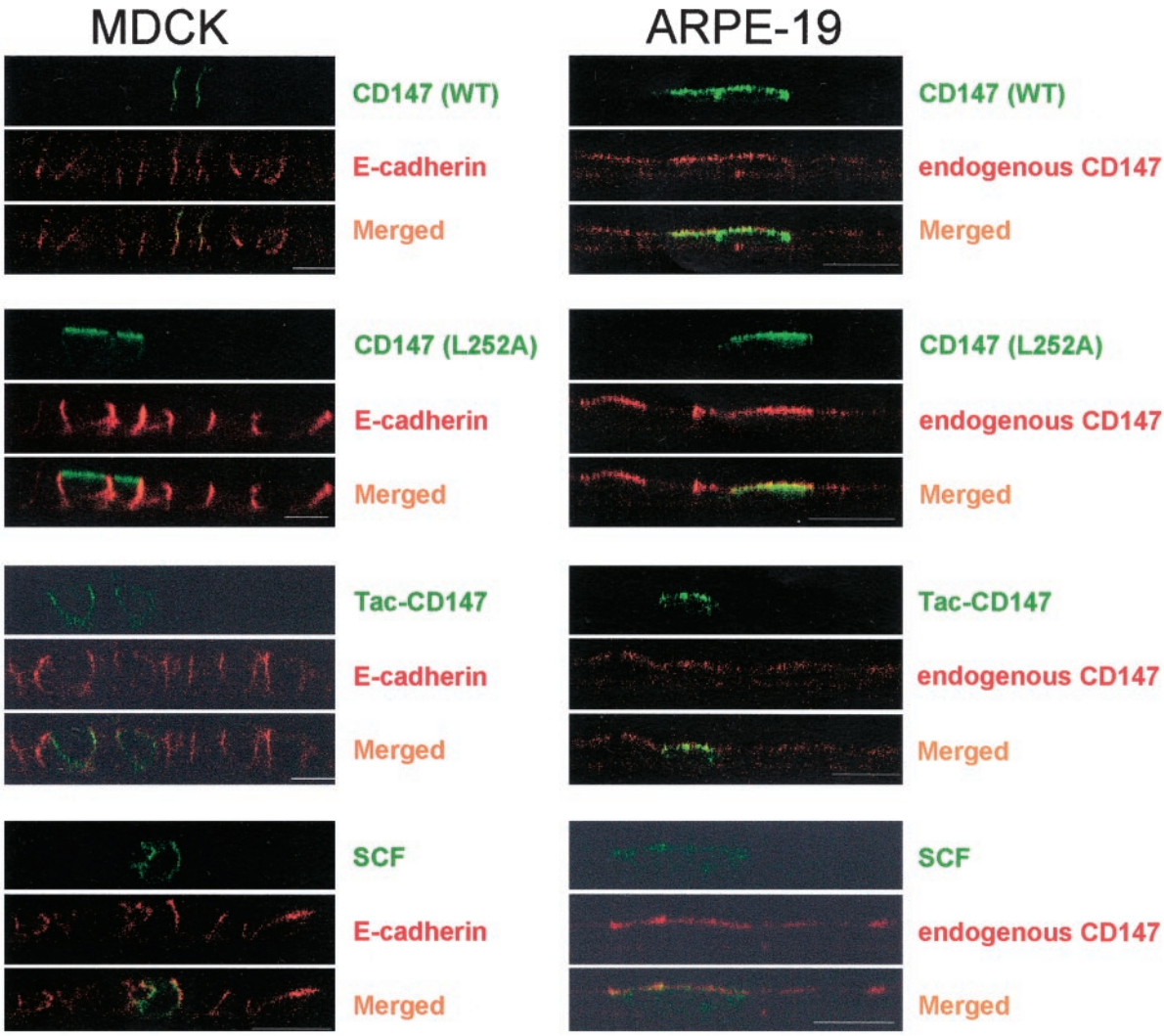

Figure 12. ARPE-19 cells do not recognize basolateral sorting motif of CD147. A vertical view (xz) of polarized MDCK and ARPE-19 monolayers transfected with various cDNAs. Immunofluorescence analysis was performed on polarized monolayer 48h posttransfection. MDCK and ARPE-19 cells were costained for E-cadherin and endogenous human CD147 respectively. ARPE-19 cells do not recognize the leucine motif of CD147 in either full-length CD147 or Tac-CD147 chimera. Bar, 10 μm.

apical signal harbored in CD147 ectodomain may affect the targeting in ARPE-19 cells, polarity of the Tac-CD147 chimera lacking CD147 ectodomain was assessed and was still found to be apical. Thus, the replacement of the CD147 ectodomain does not lead to recognition of cytoplasmic basolateral motif of CD147 in RPE. The targeting of SCF-GFP, the only other known leucine-based basolateral signal in ARPE-19 cells would have helped us extend our conclusion that the basolateral leucine motif is not recognized in RPE. However, SCF-GFP was found to be cytoplasmic in most of ARPE-19 cells with few cells expressing it apically, making it difficult to generalize our findings in such a way.

HUMAN	YEKRRKPEDVLDDDDAGSAP**L**KSSGGHQNDKGKNVRQRNSS
MOUSE	YEKRRKPDQTLDEDDPGAAP**L**KGSGTHMNDKDKNVRQRNAT
RAT	YEKRRKPDQTLDEDDPGAAP**L**KGSGSHLNDKDKNVRQRNAT
CHICKEN	YEKRRKPDEVLDDDDGGSAP**L**KSNATNHKDKNVRQRNAN
HAMSTER	YEKRRKPDQTLDEDDPGAAP**L**KGSGHHMNDKDKNVRQRNAT
ZEBRAFISH	YEKRRKPDEINDDDDSGSAP**L**KSNSATNHKDKNVRQRNSN

Figure 13. Leucine 252 (bold and underlined) is conserved in the cytoplasmic domain of CD147 across species.

Understanding how RPE cells avoid recognition of a basolateral sorting signal recognized by other epithelial cells will require in-depth analysis of expression patterns of different adaptins and of the trafficking machinery in polarized cells where they are sorted actively. The unique trafficking properties of RPE might also be attributed to the expression of different members of SNARE fusion machinery (Li *et al.*, 2002; Low *et al.*, 2002). Plasma membrane SNAREs of RPE cells will be one more tool in unraveling the molecular mechanisms responsible for the trafficking plasticity of RPE. Moreover, the environmental cues triggered by photoreceptors and interphotoreceptor matrix during developmental stages could also play a significant role in dictating trafficking pathways.

Proton-linked monocarboxylate transporter (MCT)/lactate family members are involved in transport of lactate, pyruvate, acetoacetate, and β-hydroxybutyrate. Interaction of CD147 with two members of the MCT family, namely MCT 1 and MCT4, was recently reported (Kirk *et al.*, 2000). These findings also suggest a critical role of CD147 in membrane targeting of MCTs. However this issue was not addressed in the context of polarized targeting. Intriguingly, Philp *et al.* (2003) observed loss of MCT1, MCT4, and MCT3 (RPE-specific MCT transporter) expression in the retina and the RPE of CD147 knockout mice. This critical observation made in CD147 knockout mice highlights the pivotal role of this chaperone in lactate metabolism. Hence, the knowledge of CD147's membrane targeting domain will be very useful in understanding the trafficking of MCTs.

In conclusion, we have identified a novel basolateral sorting motif in CD147 consisting of a single leucine. In the future, this sorting domain will be used as a tool to study the sorting machinery recruited in extraocular epithelial cells and the molecular machinery involved in suppressing recognition of this sorting signal in RPE.

ACKNOWLEDGMENTS

We thank Dr. Juan Bonifacino for providing us constructs encoding VHS domains of GGA1, GGA2, and GGA3 in pGAD424 vector for yeast two-hybrid analysis. This work was supported by National Institutes of Health (NIH) Grants EY08538, EY00444, EY00331, and GM34107; a Jules and Doris Stein Professorship from the Research to Prevent Blindness Foundation to E.R.B.; an NIH National Research Service Award EY14307 to A.D.; the Dolly Green Chair in Ophthalmology to D.B.; and the Dyson Foundation.

REFERENCES

Alizadeh, M., Wada, M., Gelfman, C.M., Handa, J.T., and Hjelmeland, L.M. (2001). Downregulation of differentiation specific gene expression by oxidative stress in ARPE-19 cells. Invest. Ophthalmol. Vis. Sci. *42*, 2706–2713.

Aroeti, B., Kosen, P.A., Kuntz, I.D., Cohen, F.E., and Mostov, K.E. (1993). Mutational and secondary structural analysis of the basolateral sorting signal of the polymeric immunoglobulin receptor. J. Cell Biol. *123*, 1149–1160.

Bartles, J.R., Braiterman, L.T., and Hubbard, A.L. (1985). Endogenous and exogenous domain markers of the rat hepatocyte plasma membrane. J. Cell Biol. *100*, 1126–1138.

Biswas, C., and Nugent, M.A. (1987). Membrane association of collagenase stimulatory factor(s) from B-16 melanoma cells. J. Cell Biochem. *35*, 247–258.

Biswas, C., Zhang, Y., DeCastro, R., Guo, H., Nakamura, T., Kataoka, H., and Nabeshima, K. (1995). The human tumor cell-derived collagenase stimulatory factor (renamed EMMPRIN) is a member of the immunoglobulin superfamily. Cancer Res. *55*, 434–439.

Bonifacino, J.S., and Dell'Angelica, E.C. (1999). Molecular bases for the recognition of tyrosine-based sorting signals. J. Cell Biol. *145*, 923–926.

Bonifacino, J.S., and Traub, L.M. (2003). Signals for sorting of transmembrane proteins to endosomes and lysosomes. Annu. Rev. Biochem. *72*, 395–447.

Chuang, J.Z., and Sung, C.H. (1998). The cytoplasmic tail of rhodopsin acts as a novel apical sorting signal in polarized MDCK cells. J. Cell Biol. *142*, 1245–1256.

Dunn, K.C., Aotaki-Keen, A.E., Putkey, F.R., and Hjelmeland, L.M. (1996). ARPE-19, a human retinal pigment epithelial cell line with differentiated properties. Exp. Eye Res. *62*, 155–169.

Dunn, K.C., Marmorstein, A.D., Bonilha, V.L., Rodriguez-Boulan, E., Giordano, F., and Hjelmeland, L.M. (1998). Use of the ARPE-19 cell line as a model of RPE polarity: basolateral secretion of FGF5. Invest. Ophthalmol. Vis. Sci. *39*, 2744–2749.

Fadool, J.M., and Linser, P.J. (1993a). 5A11 antigen is a cell recognition molecule which is involved in neuronal-glial interactions in avian neural retina. Dev. Dyn. *196*, 252–262.

Fadool, J.M., and Linser, P.J. (1993b). Differential glycosylation of the 5A11/HT7 antigen by neural retina and epithelial tissues in the chicken. J. Neurochem. *60*, 1354–1364.

Fan, Q.W., Yuasa, S., Kuno, N., Senda, T., Kobayashi, M., Muramatsu, T., and Kadomatsu, K. (1998). Expression of basigin, a member of the immunoglobulin superfamily, in the mouse central nervous system. Neurosci. Res. *30*, 53–63.

Finnemann, S.C., Marmorstein, A.D., Neill, J.M., and Rodriguez-Boulan, E. (1997). Identification of the retinal pigment epithelium protein RET-PE2 as CE-9/OX-47, a member of the immunoglobulin superfamily. Invest. Ophthalmol. Vis. Sci. *38*, 2366–2374.

Folsch, H., Ohno, H., Bonifacino, J.S., and Mellman, I. (1999). A novel clathrin adaptor complex mediates basolateral targeting in polarized epithelial cells. Cell *99*, 189–198.

Folsch, H., Pypaert, M., Maday, S., Pelletier, L., and Mellman, I. (2003). The AP-1A and AP-1B clathrin adaptor complexes define biochemically and functionally distinct membrane domains. J. Cell Biol. *163*, 351–362.

Frambach, D.A., Fain, G.L., Farber, D.B., and Bok, D. (1990). Beta adrenergic receptors on cultured human retinal pigment epithelium. Invest. Ophthalmol. Vis. Sci. *31*, 1767–1772.

Gan, Y., McGraw, T.E., and Rodriguez-Boulan, E. (2002). The epithelial-specific adaptor AP1B mediates post-endocytic recycling to the basolateral membrane. Nat. Cell Biol. *4*, 605–609.

Graeve, L., Drickamer, K., and Rodriguez-Boulan, E. (1989). Polarized endocytosis by Madin-Darby canine kidney cells transfected with functional chicken liver glycoprotein receptor. J. Cell Biol. *109*, 2809–2816.

Gundersen, D., Orlowski, J., and Rodriguez-Boulan, E. (1991). Apical polarity of Na,K-ATPase in retinal pigment epithelium is linked to a reversal of the ankyrin-fodrin submembrane cytoskeleton. J. Cell Biol. *112*, 863–872.

Gundersen, D., Powell, S.K., and Rodriguez-Boulan, E. (1993). Apical polarization of N-CAM in retinal pigment epithelium is dependent on contact with the neural retina. J. Cell Biol. *121*, 335–343.

Heilker, R., Spiess, M., and Crottet, P. (1999). Recognition of sorting signals by clathrin adaptors. Bioessays *21*, 558–567.

Hori, K., Katayama, N., Kachi, S., Kondo, M., Kadomatsu, K., Usukura, J., Muramatsu, T., Mori, S., and Miyake, Y. (2000). Retinal dysfunction in basigin deficiency. Invest. Ophthalmol. Vis. Sci. *41*, 3128–3133.

Hu, J., and Bok, D. (2001). A cell culture medium that supports the differentiation of human retinal pigment epithelium into functionally polarized monolayers. Mol. Vis. *7*, 14–19.

Hu, J.G., Gallemore, R.P., Bok, D., Lee, A.Y., and Frambach, D.A. (1994). Localization of NaK ATPase on cultured human retinal pigment epithelium. Invest. Ophthalmol. Vis. Sci. *35*, 3582–3588.

Hunziker, W., and Fumey, C. (1994). A di-leucine motif mediates endocytosis and basolateral sorting of macrophage IgG Fc receptors in MDCK cells. EMBO J. *13*, 2963–2967.

Igakura, T. *et al.* (1998). A null mutation in basigin, an immunoglobulin superfamily member, indicates its important roles in peri-implantation development and spermatogenesis. Dev. Biol. *194*, 152–165.

Jacob, R., Alfalah, M., Grunberg, J., Obendorf, M., and Naim, H.Y. (2000). Structural determinants required for apical sorting of an intestinal brush-border membrane protein. J. Biol. Chem. *275*, 6566–6572.

Janvier, K., Kato, Y., Boehm, M., Rose, J.R., Martina, J.A., Kim, B.-Y., Venkatesan, S., and Bonifacino, J.S. (2003). Recognition of dileucine-based sorting signals from HIV-1 Nef and LIMP-II by the AP-1 γ-σ1 and AP-3 δ-σ3 hemicomplexes. J. Cell Biol. *163*, 1281–1290.

Kasinrerk, W., Fiebiger, E., Stefanova, I., Baumruker, T., Knapp, W., and Stockinger, H. (1992). Human leukocyte activation antigen M6, a member of

the Ig superfamily, is the species homologue of rat OX-47, mouse basigin, and chicken HT7 molecule. J. Immunol. *149*, 847–854.

Kato, Y., Misra, S., Puertollano, R., Hurley, J.H., and Bonifacino, J.S. (2002). Phosphoregulation of sorting signal-VHS domain interactions by a direct electrostatic mechanism. Nat. Struct. Biol. *9*, 532–536.

Kaur, H., and Raghava, G.P. (2002a). BetaTPred: prediction of beta-TURNS in a protein using statistical algorithms. Bioinformatics *18*, 498–499.

Kaur, H., and Raghava, G.P. (2002b). An evaluation of beta-turn prediction methods. Bioinformatics *18*, 1508–1514.

Keller, P., and Simons, K. (1997). Post-Golgi biosynthetic trafficking. J. Cell Sci. *110*(Pt 24), 3001–3009.

Kirk, P., Wilson, M.C., Heddle, C., Brown, M.H., Barclay, A.N., and Halestrap, A.P. (2000). CD147 is tightly associated with lactate transporters MCT1 and MCT4 and facilitates their cell surface expression. EMBO J. *19*, 3896–3904.

Kundu, A., Avalos, R.T., Sanderson, C.M., and Nayak, D.P. (1996). Transmembrane domain of influenza virus neuraminidase, a type II protein, possesses an apical sorting signal in polarized MDCK cells. J. Virol. *70*, 6508–6515.

Le Bivic, A., Sambuy, Y., Mostov, K., and Rodriguez-Boulan, E. (1990). Vectorial targeting of an endogenous apical membrane sialoglycoprotein and uvomorulin in MDCK cells. J. Cell Biol. *110*, 1533–1539.

Le Gall, A.H., Yeaman, C., Muesch, A., and Rodriguez-Boulan, E. (1995). Epithelial cell polarity: new perspectives. Semin. Nephrol. *15*, 272–284.

Li, X., Low, S.H., Miura, M., and Weimbs, T. (2002). SNARE expression and localization in renal epithelial cells suggest mechanism for variability of trafficking phenotypes. Am. J. Physiol. Renal. Physiol. *283*, F1111–F1122.

Lin, S., Naim, H.Y., Rodriguez, A.C., and Roth, M.G. (1998). Mutations in the middle of the transmembrane domain reverse the polarity of transport of the influenza virus hemagglutinin in MDCK epithelial cells. J. Cell Biol. *142*, 51–57.

Lisanti, M.P., Caras, I.W., Davitz, M.A., and Rodriguez-Boulan, E. (1989). A glycophospholipid membrane anchor acts as an apical targeting signal in polarized epithelial cells. J. Cell Biol. *109*, 2145–2156.

Low, S.H., Marmorstein, L.Y., Miura, M., Li, X., Kudo, N., Marmorstein, A.D., and Weimbs, T. (2002). Retinal pigment epithelial cells exhibit unique expression and localization of plasma membrane syntaxins which may contribute to their trafficking phenotype. J. Cell Sci. *115*, 4545–4553.

Marmor, M.F., and Wolfensberger, T.J. (1998). The Retinal Pigment Epithelium, New York: Oxford University Press.

Marmorstein, A.D. (2001). The polarity of the retinal pigment epithelium. Traffic *2*, 867–872.

Marmorstein, A.D., Bonilha, V.L., Chiflet, S., Neill, J.M., and Rodriguez-Boulan, E. (1996). The polarity of the plasma membrane protein RET-PE2 in retinal pigment epithelium is developmentally regulated. J. Cell Sci. *109*(Pt 13), 3025–3034.

Marmorstein, A.D., Gan, Y.C., Bonilha, V.L., Finnemann, S.C., Csaky, K.G., and Rodriguez-Boulan, E. (1998a). Apical polarity of N-CAM and EMMPRIN in retinal pigment epithelium resulting from suppression of basolateral signal recognition. J. Cell Biol. *142*, 697–710.

Marmorstein, A.D., Zurzolo, C., Le Bivic, A., and Rodriguez-Boulan, E. (1998b). Cell surface biotinylation techniques and determination of protein polarity. In: Cell Biology: A Laboratory Handbook,Vol. 4, ed. J.E. Celis, New York: Academic Press, 341–350.

Matter, K., Hunziker, W., and Mellman, I. (1992). Basolateral sorting of LDL receptor in MDCK cells: the cytoplasmic domain contains two tyrosine-dependent targeting determinants. Cell *71*, 741–753.

Miller, S.S., Steinberg, R.H., and Oakley, B., 2nd. (1978). The electrogenic sodium pump of the frog retinal pigment epithelium. J. Membr. Biol. *44*, 259–279.

Miyauchi, T., Kanekura, T., Yamaoka, A., Ozawa, M., Miyazawa, S., and Muramatsu, T. (1990). Basigin, a new, broadly distributed member of the immunoglobulin superfamily, has strong homology with both the immunoglobulin V domain and the beta-chain of major histocompatibility complex class II antigen. J. Biochem. (Tokyo) *107*, 316–323.

Mostov, K.E., Verges, M., and Altschuler, Y. (2000). Membrane traffic in polarized epithelial cells. Curr. Opin. Cell Biol. *12*, 483–490.

Nehme, C.L., Cesario, M.M., Myles, D.G., Koppel, D.E., and Bartles, J.R. (1993). Breaching the diffusion barrier that compartmentalizes the transmembrane glycoprotein CE9 to the posterior-tail plasma membrane domain of the rat spermatozoon. J. Cell Biol. *120*, 687–694.

Neill, J.M., and Barnstable, C.J. (1990). Expression of the cell surface antigens RET-PE2 and N-CAM by rat retinal pigment epithelial cells during development and in tissue culture. Exp. Eye Res. *51*, 573–583.

Nelson, W.J., and Yeaman, C. (2001). Protein trafficking in the exocytic pathway of polarized epithelial cells. Trends Cell Biol. *11*, 483–486.

Ochrietor, J.D., Moroz, T.M., Kadomatsu, K., Muramatsu, T., and Linser, P.J. (2001). Retinal degeneration following failed photoreceptor maturation in 5A11/basigin null mice. Exp. Eye Res. *72*, 467–477.

Ochrietor, J.D., Moroz, T.P., Clamp, M.F., Timmers, A.M., Muramatsu, T., and Linser, P.J. (2002). Inactivation of the Basigin gene impairs normal retinal development and maturation. Vision Res. *42*, 447–453.

Odorizzi, G., and Trowbridge, I.S. (1997). Structural requirements for major histocompatibility complex class II invariant chain trafficking in polarized Madin-Darby canine kidney cells. J. Biol. Chem. *272*, 11757–11762.

Ohno, H., Aguilar, R.C., Yeh, D., Taura, D., Saito, T., and Bonifacino, J.S. (1998). The medium subunits of adaptor complexes recognize distinct but overlapping sets of tyrosine-based sorting signals. J. Biol. Chem. *273*, 25915–25921.

Ohno, H. *et al.* (1999). Mu1B, a novel adaptor medium chain expressed in polarized epithelial cells. FEBS Lett. *449*, 215–220.

Okami, T., Yamamoto, A., Omori, K., Takada, T., Uyama, M., and Tashiro, Y. (1990). Immunocytochemical localization of Na+,K(+)-ATPase in rat retinal pigment epithelial cells. J. Histochem. Cytochem. *38*, 1267–1275.

Philp, N.J., Ochrietor, J.D., Rudoy, C., Muramatsu, T., and Linser, P.J. (2003). Loss of MCT1, MCT3, and MCT4 expression in the retinal pigment epithelium and neural retina of the 5A11/basigin-null mouse. Invest. Ophthalmol. Vis. Sci. *44*, 1305–1311.

Philp, N.J., Yoon, H., and Grollman, E.F. (1998). Monocarboxylate transporter MCT1 is located in the apical membrane and MCT3 in the basal membrane of rat RPE. Am. J. Physiol. *274*, R1824–R1828.

Puertollano, R., Aguilar, R.C., Gorshkova, I., Crouch, R.J., and Bonifacino, J.S. (2001). Sorting of mannose 6-phosphate receptors mediated by the GGAs. Science *292*, 1712–1716.

Rapoport, I., Chen, Y.C., Cupers, P., Shoelson, S.E., and Kirchhausen, T. (1998). Dileucine-based sorting signals bind to the beta chain of AP-1 at a site distinct and regulated differently from the tyrosine-based motif-binding site. EMBO J. *17*, 2148–2155.

Rodionov, D.G., Nordeng, T.W., Kongsvik, T.L., and Bakke, O. (2000). The cytoplasmic tail of CD1d contains two overlapping basolateral sorting signals. J. Biol. Chem. *275*, 8279–8282.

Rodriguez-Boulan, E., and Gonzalez, A. (1999). Glycans in post-Golgi apical targeting: sorting signals or structural props? Trends Cell Biol. *9*, 291–294.

Rodriguez-Boulan, E., and Nelson, W.J. (1989). Morphogenesis of the polarized epithelial cell phenotype. Science *245*, 718–725.

Roush, D.L., Gottardi, C.J., Naim, H.Y., Roth, M.G., and Caplan, M.J. (1998). Tyrosine-based membrane protein sorting signals are differentially interpreted by polarized Madin-Darby canine kidney and LLC-PK1 epithelial cells. J. Biol. Chem. *273*, 26862–26869.

Scheiffele, P., Peranen, J., and Simons, K. (1995). N-glycans as apical sorting signals in epithelial cells. Nature *378*, 96–98.

Schlosshauer, B., and Herzog, K.H. (1990). Neurothelin: an inducible cell surface glycoprotein of blood-brain barrier-specific endothelial cells and distinct neurons. J. Cell Biol. *110*, 1261–1274.

Seulberger, H., Unger, C.M., and Risau, W. (1992). HT7, Neurothelin, Basigin, gp42 and OX-47—many names for one developmentally regulated immunoglobulin-like surface glycoprotein on blood-brain barrier endothelium, epithelial tissue barriers and neurons. Neurosci. Lett. *140*, 93–97.

Sheikh, H., and Isacke, C.M. (1996). A di-hydrophobic Leu-Val motif regulates the basolateral localization of CD44 in polarized Madin-Darby canine kidney epithelial cells. J. Biol. Chem. *271*, 12185–12190.

Simmen, T., Nobile, M., Bonifacino, J.S., and Hunziker, W. (1999). Basolateral sorting of furin in MDCK cells requires a phenylalanine-isoleucine motif together with an acidic amino acid cluster. Mol. Cell. Biol. *19*, 3136–3144.

Simonsen, A., Stang, E., Bremnes, B., Roe, M., Prydz, K., and Bakke, O. (1997). Sorting of MHC class II molecules and the associated invariant chain (Ii) in polarized MDCK cells. J. Cell Sci. *110*(Pt 5), 597–609.

Stockinger, H., Ebel, T., and Hansmann, C. (1997). CD147 (neurothelin/basigin) Workshop Panel Report. In: Leukocyte Typing VI, ed., T. Kishimoto, H. Kikutani, A.E.G.Kr.v.d. Borne *et al.,* New York: Garland Publishing, 760.

Tai, A.W., Chuang, J.Z., Bode, C., Wolfrum, U., and Sung, C.H. (1999). Rhodopsin's carboxy-terminal cytoplasmic tail acts as a membrane receptor

for cytoplasmic dynein by binding to the dynein light chain Tctex-1. Cell *97*, 877–887.

Tucker, T.A., Varga, K., Bebok, Z., Zsembery, A., McCarty, N.A., Collawn, J.F., Schwiebert, E.M., and Schwiebert, L.M. (2003). Transient transfection of polarized epithelial monolayers with CFTR and reporter genes using efficacious lipids. Am. J. Physiol. Cell Physiol. *284*, C791–C804.

Wan, L., Molloy, S.S., Thomas, L., Liu, G., Xiang, Y., Rybak, S.L., and Thomas, G. (1998). PACS-1 defines a novel gene family of cytosolic sorting proteins required for trans-Golgi network localization. Cell *94*, 205–216.

Wehrle-Haller, B., and Imhof, B.A. (2001). Stem cell factor presentation to c-Kit. Identification of a basolateral targeting domain. J. Biol. Chem. *276*, 12667–12674.

Yeaman, C., Grindstaff, K.K., and Nelson, W.J. (1999). New perspectives on mechanisms involved in generating epithelial cell polarity. Physiol. Rev. *79*, 73–98.

Yeaman, C., Le Gall, A.H., Baldwin, A.N., Monlauzeur, L., Le Bivic, A., and Rodriguez-Boulan, E. (1997). The O-glycosylated stalk domain is required for apical sorting of neurotrophin receptors in polarized MDCK cells. J. Cell Biol. *139*, 929–940.

Yoshida, S., Shibata, M., Yamamoto, S., Hagihara, M., Asai, N., Takahashi, M., Mizutani, S., Muramatsu, T., and Kadomatsu, K. (2000). Homo-oligomer formation by basigin, an immunoglobulin superfamily member, via its N-terminal immunoglobulin domain. Eur. J. Biochem. *267*, 4372–4380.

Zinn, K.M., and Marmor, M.F. (1979). The Retinal Pigment Epithelium, Cambridge: Harvard University Press.